An Actin Cross-Linking Effector of the *Vibrio* Type Six Secretion System Increases Intestinal Motility Through Macrophage Redistribution

by

JULIA SAKURA NGO

A dissertation accepted and approved in partial fulfillment of the

requirements for the degree of

Doctor of Philosophy

in Biology

Dissertation Committee:

Judith Eisen, Chair

Karen Guillemin, Advisor

Raghuveer Parthasarathy, Advisor

Matthew Barber, Core Member

Michael Harms, Institutional Representative

University of Oregon

Fall 2023

© 2023 Julia Sakura Ngo

DISSERTATION ABSTRACT

Julia Sakura Ngo

Doctor of Philosophy in Biology

Title: An Actin Cross-Linking Effector of the *Vibrio* Type Six Secretion System Increases Intestinal Motility through Macrophage Redistribution

Host-microbe interactions within the gastrointestinal tract have long been recognized as pivotal for maintaining physiological balance. However, the intricate mechanisms underlying these interactions remain enigmatic. This study delves into the complex world of host-microbe relationships, focusing on the *Vibrio* type VI secretion system (T6SS), particularly the actin cross-linking domain (ACD) of the valine-glycine repeat G (VgrG-1) protein. We explore the role of the ACD in altering intestinal motility in larval zebrafish.

Our findings reveal a fascinating mechanism underlying these interactions. *Vibrio*, known for its pathogenic potential, instigates cellular death and tissue damage within the vent region of the zebrafish intestine. This destructive action triggers an immune response within macrophages from their typical habitat in the midgut to the affected vent region.

This revelation emphasizes the disruptive influence of bacterial pathogenesis on macrophages and, by extension, their role in regulating intestinal motility. Our findings provide valuable insights into the intricacies of intestinal motility regulation in the context of host-microbe interactions.

In conclusion, this research broadens our understanding of the mechanism by which gut microbes influence host physiology, specifically in the context of intestinal motility. The presence of bacterial pathogenesis and its influence on macrophages, coupled with insights into

the intricate dynamics of host-microbe interactions, underscores the significance of this work. This intricate interplay between microbes and host systems not only reveals microbial influences on host physiology but also highlights the mechanisms employed by the host to maintain homeostasis.

CURRICULUM VITAE

NAME OF AUTHOR: Julia Sakura Ngo

GRADUATE AND UNDERGRADUATE SCHOOLS ATTENDED:

University of Oregon, Eugene
California State University, Fullerton (CSUF)

DEGREES AWARDED:

Doctor of Philosophy, Biology, 2023, University of Oregon
Bachelor of Science, Molecular Biology and Biotechnology, 2018, CSUF

AREAS OF SPECIAL INTEREST:

Microbiology

PROFESSIONAL EXPERIENCE:

Graduate Teaching Assistant, University of Oregon, September 2018 – June 2019

GRANTS, AWARDS, AND HONORS:

Raymond-Stevens Fellowship, University of Oregon, 2023

National Institutes of Health (NIH) Molecular Biology and Biophysics Training Grant Appointment, University of Oregon, 2019-2022

NIH Maximizing Access to Research Careers Training Program, CSUF, 2016-2018

Department of Biological Science Student Research Funds, CSUF, 2016-2017

Society for Advancement of Chicanos/Hispanics and Native Americans in Science Travel Award, CSUF, 2016

NIH Research Careers Preparatory Training Program, CSUF, 2015-2016

PUBLICATIONS:

Massaquoi, M.S., KongG.L., Chilin-Fuentes, D., **Ngo, J. S.,** Horve, P. F., Melancon, E., Hamilton, M. K., Eisen, J, S., & Guillemin, K., (2023). Cell-type-specific responses to the microbiota across all tissues of the larval zebrafish. *Cell Reports, 42*(2), 112095. https://doi.org/10.1016/j.celrep.2023.112095

Robinson, C.D., Sweeney, E.G., **Ngo, J.**, Ma, E., Perkins, A., Smith, T.J., Fernandez, N.L., Waters, C.M., Remington, S.J., Bohannan, B.J.M., Guillemin, K. (2021) Host-emitted amino acid cues regulate bacterial chemokinesis to enhance colonization. *Cell Host & Microbe*. https://doi.org/10.1016/j.chom.2021.06.003

Medina, M., Rizo, A., Dinh, D., Chau, B., Omidvar, M., Juarez, A., **Ngo, J.,** Johnson, HA. (2018) MopA, the Mn oxidizing protein from *Erythrobacter* sp. SD-21, requires heme and NAD+ for Mn(II) oxidation. *Frontiers in Microbiology*. http://doi.org/10.3389/fmicb.2018.02671

ACKNOWLEDGMENTS

I would like to express my deepest gratitude to my mentors, Dr. Karen Guillemin and Dr. Raghuveer Parthasarathy, for their unwavering support and guidance throughout my academic journey. Their mentorship has been instrumental in shaping my research and personal growth, and I am truly fortunate to have had the opportunity to learn from them.

I am immensely thankful to all the members of both research labs for their camaraderie and support. Their encouragement during those challenging moments in the lab, whether it was sharing a lunch break or lending a helping hand to unlock the lab doors, made a significant difference in my research experience.

I would like to express my sincere appreciation to Jonah Sokoloff for his invaluable assistance during our research endeavors. His collaboration in carrying out key experiments in tandem with me was instrumental in enabling us to maximize our data collection during the limited time we had. Jonah's dedication and support greatly contributed to the success of our research, and I am grateful for his contributions.

I would also like to extend my heartfelt thanks to my thesis committee, Drs. Judith Eisen, Mike Harms, and Matt Barber, for their unwavering support throughout this research journey. Their guidance, patience, and expertise were instrumental in shaping the direction of my project.

To my parents, I owe a debt of gratitude for their constant support and motivation. Their care packages, filled with instant ramen and love, sustained me during the long hours of research and writing. Their belief in my abilities had been a driving force throughout my academic journey.

This dissertation is dedicated to my friends and family whose support and encouragement have been my constant source of strength throughout this academic journey.

TABLE OF CONTENTS

LIST OF FIGURES

Figure Page

CHAPTER I

INTRODUCTION

Microbial Influence on Host Physiology

In recent years, the profound influence of microbes on host health has become increasingly apparent. From a myriad of microbial and anti-microbial products lining our supermarket shelves, the notion of microbes significantly impacting host physiology and improving human health is no longer confined to the realm of scientific inquiry. While the general populace has embraced this concept, the specific mechanisms behind these host-microbe interactions continue to remain shrouded in mystery.

This intricate interplay between microbes and their host organisms remains one of the most fascinating and enigmatic fields of study in contemporary biology. Due to their high abundance in the intestine, gut microbes exert a profound influence on host physiology, impacting a range of critical processes. Microbial factors that impact host physiology can be classified broadly into 1) microbial cues that are made by microbes for their own survival and recognized by host detection systems and 2) microbial signals produced by microbes to target host processes, such as toxins and secreted effector proteins.

Microbial cues include essential components of bacterial cells that are recognized by innate immune receptors and have been termed either pathogen or microbe-associated molecular patterns (PAMPs/MAMPs) (Janeway, 1989). For example, flagellin, an essential component of bacterial flagella, is recognized by the Toll-like receptor 5 (TLR5) on epithelial and immune cells triggering pro-inflammatory responses and increasing the risk of chronic inflammation (Carvalho et al., 2012). Lipopolysaccharides (LPS), an integral component of the outer

membrane of most Gram-negative bacteria, is recognized by TLR4, inducing the release of pro-inflammatory cytokines (McAleer & Vella, 2008). Another bacterial cell wall MAMP, peptidoglycan, is recognized by cell surface TLR2 and cytoplasmic NOD receptors to induce pro-inflammatory cytokines (Zhao et al., 2011).

Another class of microbial cues that elicit host responses are short chain fatty acids (SCFA), the products of bacterial fermentation of complex polysaccharides. SCFAs that are known to play a role in host health and disease are acetate, propionate and butyrate, which are produced by a wide variety of colonic bacteria and serve as essential energy sources for host enterocytes (Fitch & Fleming, 1999; Wong et al., 2006). Additionally, these SCFAs have been shown to play a role in neuroendocrine function through G protein coupled receptor binding on enteroendocrine cells (Brown et al., 2003; Samuel et al., 2008).

The consequences of host detection of microbial cues are highly dependent on the specific microbial cues detected, the host cells that detects these cues, and the location of detection. In animals, a critical interface of microbial-host interactions is the intestinal epithelial surface (Ha et al., 2014). Here, cell types such as macrophages, neutrophils, and enteric neurons that regulate intestinal motility sense and respond to microbial cues (Muller et al., 2014; Rolig et al., 2015).

The second broad class of microbial factors that impact host physiology are effectors that specifically target host cellular functions. One such example is Cholera Toxin (CT), a heterodimeric protein secreted by *Vibrio cholerae*. *Vibrio*, a Gram-negative aquatic bacterium well known for its ability to influence host physiology (Breen et al., 2021; Chowdhury et al., 2016). *Vibrio's* most notorious impact on human health is as the cause of cholerae, a diarrheal

disease responsible for high infant mortality in western Africa and southeast Asia (Vanden Broeck et al., 2007). Different Vibrio isolates have different toxin contents, with CT being specific to toxigenic serogroups 01 and 0139 *Vibrio* and not present in nontoxigenic or environmental *Vibrio* strains, some of which have been linked to gastroenteritis (Chatterjee et al., 2009; Pang et al., 2007; Schwartz et al., 2019).

CT exerts its molecular activity by acting as a potent activator of adenylate cyclase upon entering host cells (Clemens et al., 2017). This activation leads to an uncontrolled increase in cyclic AMP levels within the host cell, ultimately disrupting ion transport mechanisms in the intestinal epithelium (Clemens et al., 2017). The physiological consequences of this molecular action is profuse diarrhea and dehydration, as the disrupted ion transport leads to the secretion of large volumes of electrolyte-rich fluids into the gut lumen (Clemens et al., 2017). Paradoxically, this severe diarrheal symptom can benefit the pathogen by increasing its changes of transmission, as the infected individual sheds copious amounts of pathogen containing stool into the environment, further facilitating the spread of *Vibrio cholerae* to new hosts (Clemens et al., 2017).

In addition to secreted microbial signals, microbes can target host processes by the delivery of effector proteins through secretion systems. These include the flagellar-like Type III secretion system (T3SS), the conjugative pilus-like Type IV secretion system (T4SS), and the phage tail-like Type VI secretion system (T6SS) (Green & Mecsas, 2016). The latter is the focus of this dissertation and discussed in more detail below.

The *Vibrio* Type VI Secretion System and Its Impacts on the Host

The *Vibrio* T6SS was first described in an environmental *Vibrio* isolate (Pukatzki et al., 2006). The presence of intact T6SS gene clusters in both toxigenic and nontoxigenic *Vibrio* strains suggests that this system plays a pivotal role in persistence within hosts and environmental niches (Miyata et al., 2010). Notably, in the zebrafish intestine, the T6SS is not required for colonization; however, it contributes to the modulation of the zebrafish microbiome and the induction of mucin secretion, a hallmark of diarrhea (Breen et al., 2021; Logan et al., 2018).

The T6SS comprises three main categories of genes: structural, regulatory, and effector components (Miyata et al., 2010). Regulatory elements are essential for the T6SS's function, ensuring proper operation (Pukatzki et al., 2006). Structural components form the secretion apparatus, make up the membrane complex, the tail, the tail tube/sheath, and the spike complex (Cherrak et al., 2019). Effector components of the T6SS are translocated into target prokaryotic and eukaryotic cells through contact-dependent mechanisms, exerting diverse effects such as actin cross-linking, cell wall degradation, and the targeting of cellular membranes and nucleic acids (Monjarás Feria & Valvano, 2020; Pukatzki et al., 2007a; Sana et al., 2017).

A specific T6SS protein that is the focus of my research is the valine-glycine repeat G (VgrG-1) protein, serves as both a structural and effector component (Cherrak et al., 2019; Pukatzki et al., 2007a). There are three types of VgrG proteins-VgrG-1, VgrG-2 and VgrG-3-that come together to form a trimeric complex akin to the gp27 and gp5 proteins of the bacteriophage T4 tail spike and are a part of the T6SS spike complex (Cascales, 2008; Cherrak et al., 2019; Pukatzki et al., 2007a). While these proteins share a homologous N-terminal region that

facilitates their interaction, they each encode distinct C-terminal domains, known as their effector domains (Pukatzki et al., 2007a). VgrG-2 serves solely as a structural component, while VgrG-3 contains a peptidoglycan binding domain used to hydrolyze the cell walls of Gram-negative bacteria (Brooks et al., 2013; Pukatzki et al., 2007a). In contrast, VgrG-1 encodes an actin cross-linking domain (ACD), which is a eukaryotic effector domain (Pukatzki et al., 2006, 2007a).

The ACD: A Dual Agent of Destruction and Influence

The ACD of VgrG-1 bears significant homology to the ACD of the well-studied RtxA (Repeats in ToXin), and it exhibits a similar mechanism for cross-linking cytosolic monomeric G-actin (Durand et al., 2012). The VgrG-1 ACD demonstrates a cytotoxic effect when internalized by eukaryotic cells, specifically in the amoebae *Dictyostelium discoideum* and in cultured murine macrophages, suggesting that it targets phagocytic cell types (Ma & Mekalanos, 2010a; Pukatzki et al., 2006, 2007a). However, the activity of the ACD is not limited to cellular destruction, but it also mediates complex host immune responses. In the context of the mouse intestine, the ACD has been shown to induce various responses including fluid accumulation, inflammation characterized by cellular infiltration, and upregulation of inflammatory gene expression, as well as actin cross-linking in macrophages that were extracted from the intestine of infected mice (Ma & Mekalanos, 2010a). Interestingly, within the zebrafish intestine, the VgrG-1ACD drives heightened intestinal contractility, culminating in the expulsion of a commensal bacterial strain, *Aeromonas*, exemplifying its diverse effects across different host organisms (Logan et al., 2018). This dual agent of destruction and influence in *Vibrio* physiology sets the stage for our investigation.

Macrophages and Their Role in Gut Motility

The macrophage targeting of *Vibrio's* ACD and its impact on intestinal motility are intriguing in light of emerging research on macrophages' involvement in the regulation of intestinal motility. In the murine model, a distinctive subset of macrophages, known as muscularis macrophages, located within the intestinal muscularis externa, are key regulators of intestinal motility. These macrophages engage in specialized communication with the enteric neurons of the enteric nervous system encircling the intestine (Muller et al., 2014). They express bone morphogenetic protein 2 (BMP2) which serves to perpetually activate enteric neurons expressing the BMP receptor (BMPR) (Muller et al., 2014). In return, enteric neurons express colony stimulating factor 1 (CSF1), a growth factor vital for macrophage development (Muller et al., 2014; Sehgal et al., 2021). Intriguingly, antibiotic depletion of intestinal microbes has revealed that the microbiota exerts a level of control over CSF1 expression by enteric neurons, thereby influencing macrophage population and BMP2 production (Muller et al., 2014). Notably, the addition of LPS or the introduction of microbiota through fecal transfers to antibiotic-treated mice rescued CSF1 expression and the macrophage population, highlighting the capacity of luminal microbes to influence the macrophage-neuronal crosstalk that governs intestinal motility (Muller et al., 2014).

In the zebrafish model, the discovery of muscularis macrophages has further illuminated these intriguing interactions (Graves et al., 2021). These muscularis macrophages have been found to closely associate with neural projections in both adult and larval fish, suggesting a semblance of immune-nervous system interactions in the intestinal milieu similar to the murine model (Graves et al., 2021). The specification of these macrophages requires the function of the

transcription factor Interferon regulatory factor 8 (Irf8) (Shiau et al., 2015). Strikingly, depletion of these muscularis macrophages in *irf8* deficient larval zebrafish was found to induce altered intestinal motility, specifically a decrease in the transit time of intestinal contents, indicating their pivotal role in the regulation of intestinal motility (Muller et al., 2014). An interesting facet of these macrophages is their role as the primary source of the complement component C1q protein in the intestines of both mice and zebrafish, which initiates the classical complement pathway vital for immune defense (Earley et al., 2018; Noris & Remuzzi, 2013; Pendse et al., 2023; Son et al., 2015).

The complex network of interactions between different cell types within the intestine, along with their responses to luminal microbes, can shape organ-wide phenomena such as intestinal motility and bacterial competitive interactions. Understanding these intricate connections is vital to gaining a more comprehensive picture of host-microbe interplay and how it shapes the homeostasis of the intestinal environment.

Our study seeks to unravel how the ACD alters intestinal motility in zebrafish. By delving into the specifics of this interaction, we aim not only to broaden our understanding of the microbial influences on host physiology but also gain insight into the intricate mechanisms underlying host-microbe interactions. This research contributes to a comprehensive knowledge of the organ-wide consequences of local bacterial-host cell interactions and offers new perspectives on how infections can contribute to gastrointestinal pathologies such as intestinal dysmotility.

CHAPTER II

AN ACTIN CROSS-LINKING EFFECTOR OF THE *VIBRIO* TYPE SIX SECRETION SYSTEM INCREASES INTESTINAL MOTILITY THROUGH MACROPHAGE REDISTRIBUTION

Introduction

Bacterial colonizers of animals shape the tissues in which they reside to confer colonization advantages. *Vibrio cholerae* colonization of the intestine causes dramatic changes to the tissue which are thought to promote the bacteria's persistence within the host and facilitate its transmission to new hosts (Hsiao & Zhu, 2020). The study of host immune responses to pathogens like *Vibrio* unveils a rich tapestry of interactions that provide insights in to how such pathogens are able to colonize and persist within the host (Sit et al., 2022). By delving into these host-pathogen dynamics, we gain a deeper understanding of the colonization and persistence strategies employed by these pathogens and the effects they have on their host environments.

We have used the larval zebrafish, a model organism amenable to live imaging and genetic manipulations, to investigate the dynamics of *Vibrio* intestinal colonization and competition with other gut bacteria, using both the human clinical *V. cholerae* isolate El Tor strain C6706 and a zebrafish *V. cholerae* isolate ZWU0020 (Logan et al., 2018; Stephens et al., 2015; Wiles et al., 2016, 2020). We discovered that the zebrafish *Vibrio* isolate is highly motile within the intestine, a trait that allowed it to resist host intestinal motility at the expense of a more susceptible rival *Aeromonas* species (Wiles et al., 2016, 2020). These intricacies were first observed in *Vibrio* ZWU0020 (Z20), when paired with a functional enteric nervous system in zebrafish, this *Vibrio* species assumes the role of an eviction artist, effectively removing an

initially colonized *Aeromonas* strain from the gut (Wiles et al., 2016). Further explorations with the *V. cholerae* El Tor strain C6706 revealed that it promoted *Aeromonas* expulsion by enhancing the strength of host intestinal contractions through its Type VI secretion system (T6SS) (Logan et al., 2018).

The bacterial T6SS functions as a contact-dependent secretion system used to deliver effector proteins into target cells (Basler et al., 2013; Ma et al., 2009). Although the T6SS is capable of targeting both prokaryotic and eukaryotic cells, it has been mainly characterized for its antimicrobial properties such as cell wall degradation, cell membrane disruption, and nucleic acid destruction (Russell et al., 2014). Given the role of *Vibrio* T6SS in eliminating *Aeromonas* from the zebrafish intestine, it was surprising to find that was mediated via the actin cross-linking domain (ACD) within the valine-glycine repeat G (VgrG-1) effector protein of the *Vibrio* Type VI Secretion System (T6SS). The VgrG-1 protein encodes a 395 amino acid C-terminal domain, which acts as a structural component of the T6SS, and harbors the eukaryotic effector ACD (Pukatzki et al., 2007a). Additional support for the eukaryotic specificity of the ACD comes from its dispensability in, contact-dependent T6SS killing of *Aeromonas* by *Vibrio* (Logan et al., 2018).

Specifically, the ACD has been implicated in *Vibrio cholerae* impairment of phagocytic activity, and, eventually the death of cultured macrophages, as well as macrophages extracted from infant mice (Durand et al., 2012; Ma & Mekalanos, 2010a; Pukatzki et al., 2007a). In the mouse model, the ACD induces fluid accumulation and inflammation by promoting immune cell infiltration, as measured in dissected intestines of infected mice (Ma & Mekalanos, 2010a).

Notably, macrophages have emerged as key players in the regulation of intestinal motility through constitutive signaling of bone morphogenetic protein 2 (BMP2) and complement component C1q to enteric neurons (Muller et al., 2014; Pendse et al., 2023). In the context of zebrafish, macrophages originating from *irf8*-specified cell lineages have been identified as regulators of intestinal motility during larval developmental stages as mutant fish lacking the *irf8* gene showed decreased transit time of food (Graves et al., 2021).

Based on the existing literature, we postulate that the ACD encoded by the *Vibrio* T6SS may target and induce macrophage death in larval zebrafish to increase intestinal contractility, thus, our primary objective in this study was to investigate this hypothesis. We investigated how the *Vibrio* T6SS ACD exerts its effect on intestinal motility. We show that the native zebrafish *Vibrio* Z20, like the human *V. cholerae* El Tor strain C6706, increases the strength of gut contractions and displaces *Aeromonas* through a T6SS ACD dependent mechanism. We show that macrophages are involved in this increased intestinal motility and that in macrophage-depleted animals, intestinal gut contractions are indistinguishable between larvae infected with wild type or ACD-deficient *Vibrio*. We find that this effect on macrophages is not due to ACD-dependent macrophage killing, but rather that ACD-induced intestinal tissue damage predominantly in the posterior region of the intestine orchestrates the redistribution of macrophages away from their even distribution in proximity with enteric neurons along the length of the intestine. This indirect effect on intestinal motility by the pathological redistribution of macrophages provides a new paradigm for intestinal dysmotility in inflammatory gastrointestinal disorders.

Results

ACD-Mediated Effects on Tissue Damage and Intestinal Motility in Larval Zebrafish

The zebrafish-isolate *Vibrio* strain ZWU0020 (Z20), despite lacking the cholera toxin, induces tissue damage in zebrafish larvae. To characterize these pathogenic effects, we inoculated flasks housing germ-free (GF) zebrafish with Z20 at 4 days post-fertilization (dpf). Starting at 13 hours post-inoculation (hpi) we conducted imaging sessions at 20-minute intervals over 13 hours to investigate alterations in gut morphology. We observed and quantified three types of intestinal damage which were visually evident in the images captured overnight (Figure 1A). The initial observation focused on was the vent's widening, as it presented the most noticeable change over time, as depicted in Figure 1A. This measurement was quantified as vent width which increased over time (Figure 1B) and is denoted by the black bracket in Figure 1A. Additionally, we observed a progressive expansion of the distal gut, quantified as gut width (Figure 1C), with its measurement point indicated by the black arrowhead in Figure 1A. Our final measurement of pathogenic effects involved determining the gut length (Figure 1D), measured from the intestinal bulb to the vent, following the path of the intestinal lumen. Intriguingly, we observed a reduction in the gut length overtime, which contrasted with the trends observed in the other two measurements. Although the most pronounced gut shrinking occurs between 13 and 17 hpi, the widening of the vent and gut exhibit a more gradual trend, with similar patterns of increase over time. These observations indicate substantial tissue damage, with noticeable swelling at the distal end of the gut accompanied by a reduction in gut length.

To test whether the observed alteration in gut morphology were attributed to the presence of the actin crosslinking-domain (ACD), a known eukaryotic effector, we performed targeted genetic manipulations (Ma & Mekalanos, 2010b). Specifically, we deleted the ACD from the VgrG-1 protein of Z20, generating an ACD-deficient mutant strain, $Z20^{\Delta ACD}$ using previously described methods (Wiles et al., 2018, 2020). GF fish were inoculated with either their parental microbiota, Z20 or $Z20^{\Delta ACD}$ at 5 dpf and vents were imaged and analyzed at 24 hpi and 6 dpf. We compared vent sizes among various experimental groups, including conventionalized (CVZ) fish, which experienced the GF derivation process but were subsequently raised with their parental microbiota, GF fish, Z20 mono-associated fish, and $Z20^{\Delta ACD}$ mono-associated fish. Notably, the observed increase in vent width was a distinctive feature exhibited solely by fish that were mono-associated with Z20 (Figure 1F).

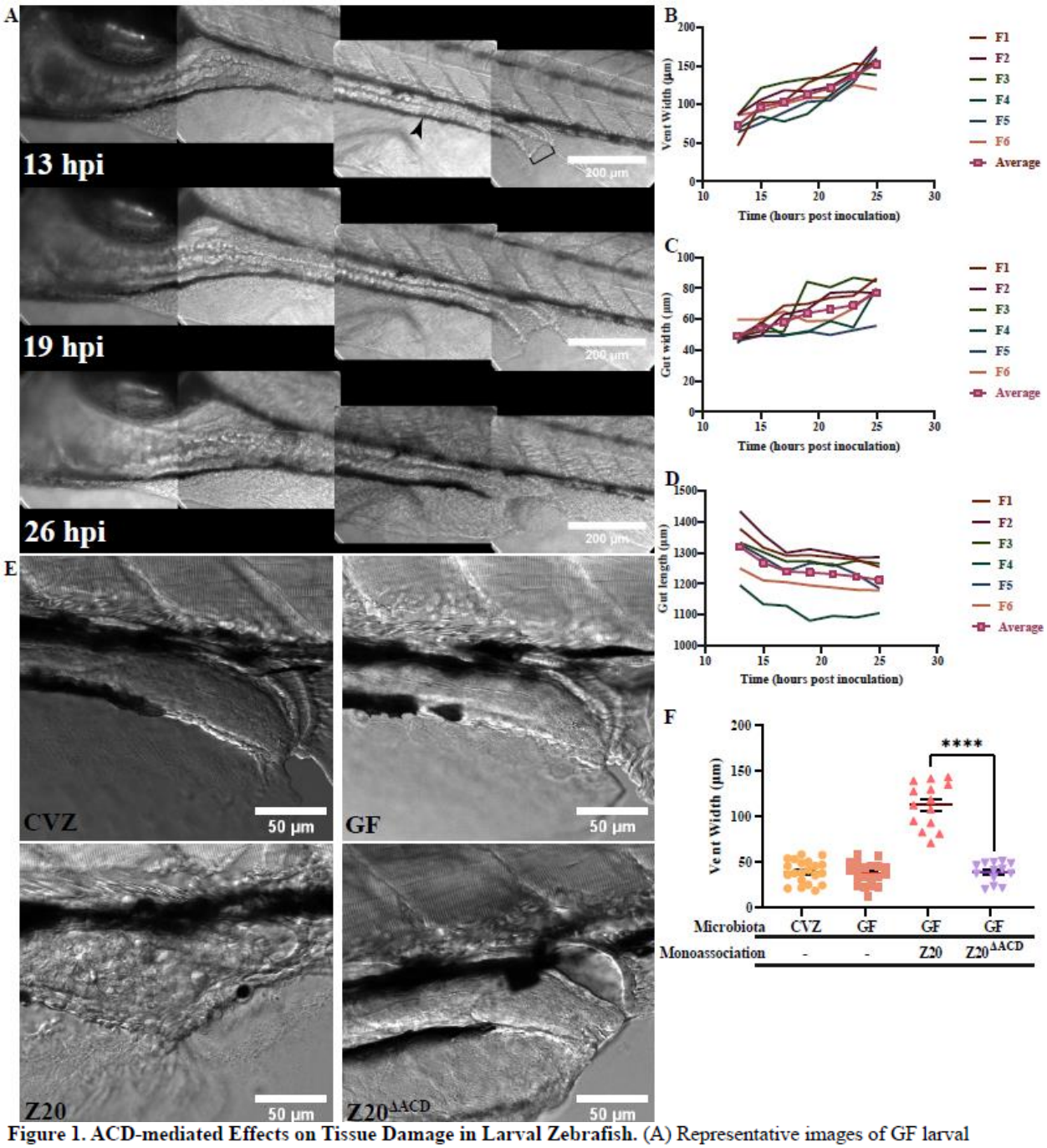

Figure 1. ACD-mediated Effects on Tissue Damage in Larval Zebrafish. (A) Representative images of GF larval zebrafish monoassociated with Z20 (scale bar 200 µm). (B) Measurement of zebrafish vent width from 13 hpi to 25 hpi under the same conditions as in (A), black bracket in (A) indicates vent. Six fish measured with the average plotted with pink boxes. (C) Measurement of posterior zebrafish gut width from 13 hpi to 25 hpi under the same conditions as in (A), black arrowhead indicates location of measurement. (D) Measurement of zebrafish gut length from 13 hpi to 25 hpi under the same conditions as in (A), measurement was made following the gut lumen. (E) Representative images of GF larval zebrafish conventialized (CVZ) or mono-associated with Z20 or $Z20^{\Delta ACD}$ taken on a Leica SPE confocal microscope (scale bar 50 µm). (F) Measurement of zebrafish vent width in microns. A significant difference in vent width comparing fish monoassociated with Z20 to fish monoassociated with $Z20^{\Delta ACD}$ is detected (*unpaired t test* ($P < 0.0001$).

Prior work has shown that the human pathogen Vibrio cholerae has an ACD-dependent ability to enhance the strength of gut contractions, as described in the Introduction (Logan et al., 2018). To ascertain whether the ACD of zebrafish-derived Z20 has a similar capability, we quantified the strength of intestinal contractions as in previous work (Logan et al., 2018). By 4 dpf zebrafish intestines exhibit periodic propagative contractions that can propel dense aggregates through the gut (Holmberg et al., 2007; Wiles et al., 2016). In brief, we captured movies of a roughly 400 micron long segment of the posterior intestine of live fish, outlined in Figure $2A_1$, using differential interference contrast (DIC) microscopy for 5 minute durations at 5 frames per second. We performed image velocimetry techniques on these images, assessing the frequency and the amplitude of periodic contractions as in prior work (Figure $2A_2$) (Ganz et al., 2018; Logan et al., 2018; Wiles et al., 2016). Fish mono-associated with Z20 displayed larger image velocimetry vectors than those mono-associated with $Z20^{\Delta ACD}$, a phenomenon analogous to the effects of *Vibrio cholerae* on zebrafish intestines (Figure 2 A_2) (Logan et al., 2018). These measurements revealed that fish mono-associated with Z20 exhibit gut amplitudes that are roughly 100% greater than those mono-associated with $Z20^{\Delta ACD}$ (Figure 2B). Notably, the frequency of periodic gut contractions did not differ between the two conditions (Figure 2B).

Previously it had been demonstrated that Z20 has the ability to expel a commensal bacterial species, *Aeromonas* strain ZOR0001 (*Aeromonas*), from the zebrafish gut (Wiles et al., 2016). It was demonstrated that in the *Vibrio cholerae* strain C6706, the expulsion of *Aeromonas* was attributed to the action of the ACD (Logan et al., 2018). However, the precise mechanism behind how Z20 accomplishes this *Aeromonas* expulsion was still unclear, but we were confident that it would be similar, considering the resemblance of Z20's 16S rRNA gene sequence to that

of *Vibrio cholerae* (Wiles et al., 2016). We quantified total bacterial abundance by using gut dissection and standard plating techniques. In mono-association *Aeromonas* populations reached slightly above 10^4 colony-forming units (CFU) per gut (Figure 2E). Following a 24-hour challenge by Z20, established *Aeromonas* populations decreased by approximately 10-fold (Figure 2E). As anticipated, *Aeromonas* populations challenged by $Z20^{\Delta ACD}$ for 24 hours exhibited similar abundances to the mono-association (Figure 2E). Notably, in the zebrafish, the mutant $Z20^{\Delta ACD}$ colonized the intestine at levels comparable to those of the WT Z20 in these challenge scenarios, reaching abundances of 10^5 CFU per gut (Figure 2E). In this study, we reveal that the ACD plays a pivotal role in Z20's ability to expel *Aeromonas*, as is the case with *Vibrio cholerae* (Figure 2E).

These results collectively highlight the ACD-mediated effects on tissue damage, intestinal motility, and competitive interactions in larval zebrafish, shedding light on the mechanisms underlying these phenomena.

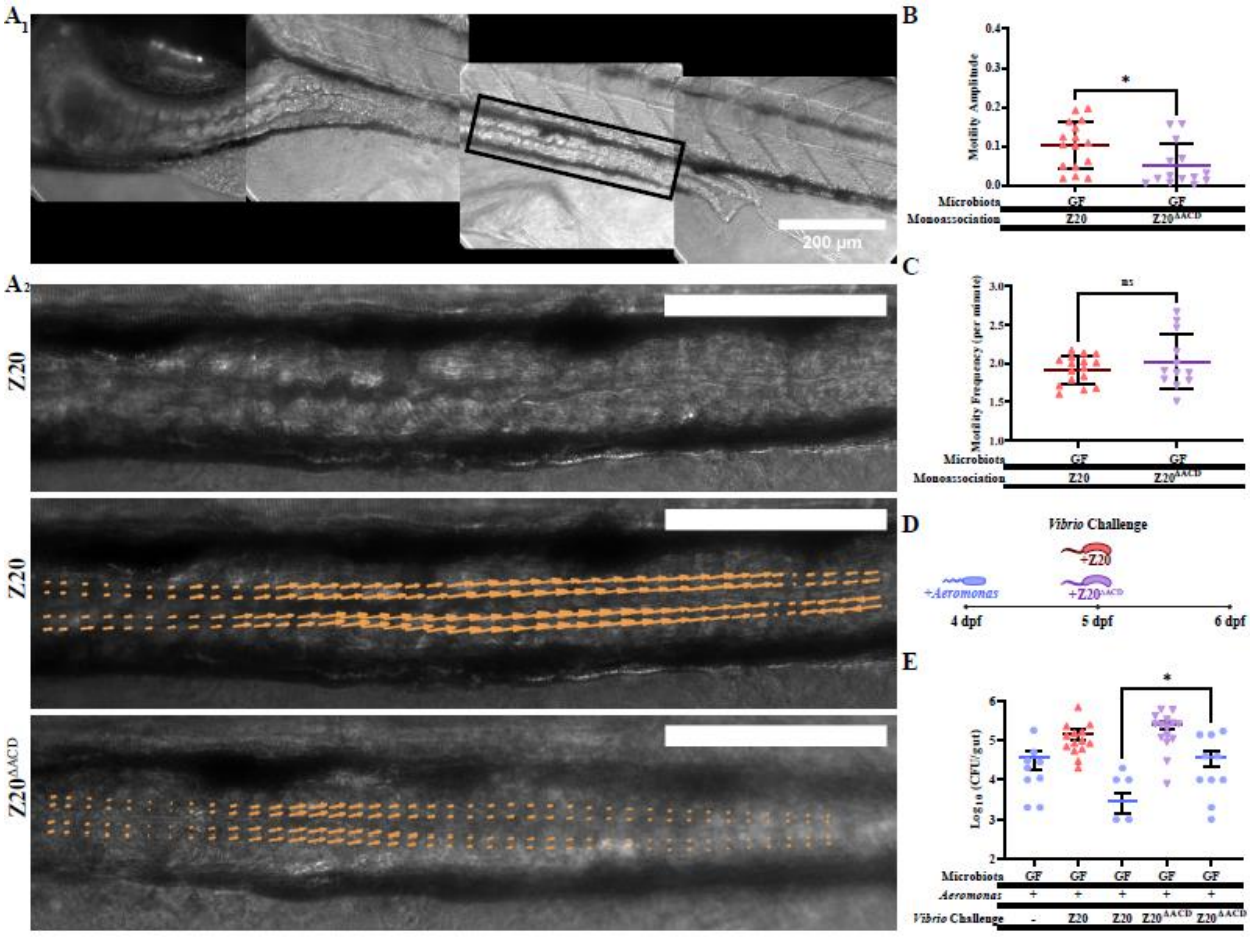

Figure 2. ACD-mediated Effects on Intestinal Motility in Larval Zebrafish. (A) A_1: Representative images of GF larval zebrafish monoassociated with Z20 at 13 hpi, black rectangle indicated area imaged for gut motilty measurements (scale bar 200 µm). A_2: Representative single frames from a 5-minute movie of zebrafish intestines from GF larval zebrafish mono-associated with Z20 or $Z20^{\Delta ACD}$, with superimposed arrows indicaiting local image velocity. The proportionality between velocity and arrow length is the same for each image, and each is from a timepoint at approximately the peak of an intestinal contraction. (B) Gut motility amplitudes for fish under the same conditions as in (A). Fish mono-associated with Z20 exhibit higher gut amplitudes compared to those mono-associated with $Z20^{\Delta ACD}$ (*Mann-Whitney U test, P = 0.0138*). (C) Frequency of periodic gut motility of fish under the same conditions as in (A). The distributions of gut motility frequencies are comparable, with no statistically significant difference (*Mann-Whitney U test, P = 0.7358*). (D) Schematic representation of the *Vibrio* challenge protocol used to investigate *Aeromonas-Vibrio* interactions. *Aeromonas* colonization of GF larvae at 4 dpf is followed by the introduction of Z20 or $Z20^{\Delta ACD}$ at 5 dpf for 24 hours, before abundances are quantified through dissections and serial plating at 6 dpf. (E) Abundances of *Aeromonas* (blue hexagons), Z20 (red triangles), and $Z20^{\Delta ACD}$ (purple inverted triangles) after mono-association and challenges. Statistically significant differences in *Aeromonas* abundances following Z20 challenges are observed compared to abundances following $Z20^{\Delta ACD}$ challenges (*unpaired t test, P = 0.0416*).

Macrophage Depletion Enhances Intestinal Contraction Strength

In culture, macrophages have been shown to be susceptible to ACD-mediated killing, thus making them the predicted natural targets of the ACD in a host organism (Ma et al., 2009; Pukatzki et al., 2006, 2007b). Intriguingly, *irf8* derived macrophages have been demonstrated to regulate intestinal motility in larval zebrafish (Graves et al., 2021). Consequently, our research focused on investigating the role of macrophages in the ACD-mediated alterations to intestinal motility. To accomplish this we employed the Clustered Regularly Interspace Short Palindromic Repeats (CRISPR)-Cas9 gene editing system to target the *irf8* gene (Keatinge et al., 2021). *Tg(mpeg:mCherry)* embryos were injected at the single cell stage with a mixture containing the Cas9 enzyme and single guide RNAs (sgRNA) designed to target the *irf8* gene. Once injected, Cas9, often referred to as "molecular scissors", is guided by the sgRNA to the *ifr8* gene (Hillary & Ceasar, 2023). At the target location, Cas9 cuts the DNA in the *irf8* gene (Hillary & Ceasar, 2023). When the cell's natural repair machinery fixes this cut, it can lead to the addition of deletion of specific genetic information, effectively altering the function of the gene (Hillary & Ceasar, 2023). Working with F0 crispants, zebrafish larvae injected with the CRISPR-Cas9 system, offers an advantage compared to other methods of gene editing, such as morpholinos, which are constrained by their limited time frame of approximately 3 dpf (Bill et al., 2009). In contrast, the F0 crispant approach facilitates rapid and efficient genetic manipulation in the first generation (Kroll et al., 2021). This is a stark contrast to the time-consuming process of generating homozygous mutants, which can take up to four to six months to achieve (Sorlien et al., 2018). The F0 crispant method thus stands out as a valuable tool for streamlined and effective genetic research in zebrafish.

To explore the influence of macrophages in ACD-mediated alterations of intestinal motility, we employed *tg(mpeg:mCherry)* embryos, which were subjected to injection of the CRISPR-Cas9 mixture at the single-cell stage, generating F0 crispants (Δ*irf8*). These crispants were compared to uninjected control fish as depicted in Figure 3A. Our analysis of macrophage cell counts across the entire image captured in Figure 3A revealed that Δ*irf8* fish have approximately 25% fewer macrophages in comparison to control WT fish (Figure 3B).

It has been previously shown that larval zebrafish lacking the *irf8* gene have decreased intestinal transit time of solid food compared to WT siblings (Graves et al., 2021). However, the relationship of transit time to intestinal mechanics is not straightforward, as it may depend on the frequency of contractions, their strength, their coherence, and more. Our study involved comparing the intestinal movements of GF and conventional, fish that did not go through the GF derivation, (CV) Δ*irf8* fish and WT fish. Notably, Δ*irf8* fish displayed higher gut contraction amplitudes regardless of the microbiota (Figure 3C). Therefore, we combined the data ignoring the microbiota for a more comprehensive analysis and found that Δ*irf8* fish exhibited approximately a 70% increase in contraction amplitude compared to WT fish (Figure D). Similar to WT fish mono-associated with Z20, Δ*irf8* fish exhibited larger image velocimetry vectors than WT fish (Figure $2A_2$). Despite the increased gut contraction strength in Δ*irf8* fish, the was no detectable difference in the distributions of gut motility frequencies (Figure 3E).

To test macrophage necessity on ACD-mediated alterations to intestinal motility, Δ*irf8* fish were derived germ-free and mono-associated with either *Vibrio* Z20 or $Z20^{\Delta ACD}$. For both sets, we found gut contraction amplitudes that were similar to each other, and similar to the Δ*irf8* fish in the absence of *Vibrio* (Figure 3F), implying that depletion of macrophages maximizes the

strength of gut contractions and the *Vibrio* ACD does not induce significant macrophage-independent gut motility changes. Again, we found that the distribution of gut motility frequencies did not show differences between conditions (Figure 3G).

These results collectively demonstrate that macrophage depletion enhances intestinal contraction strength in larval zebrafish, with implications for the regulation of gut motility.

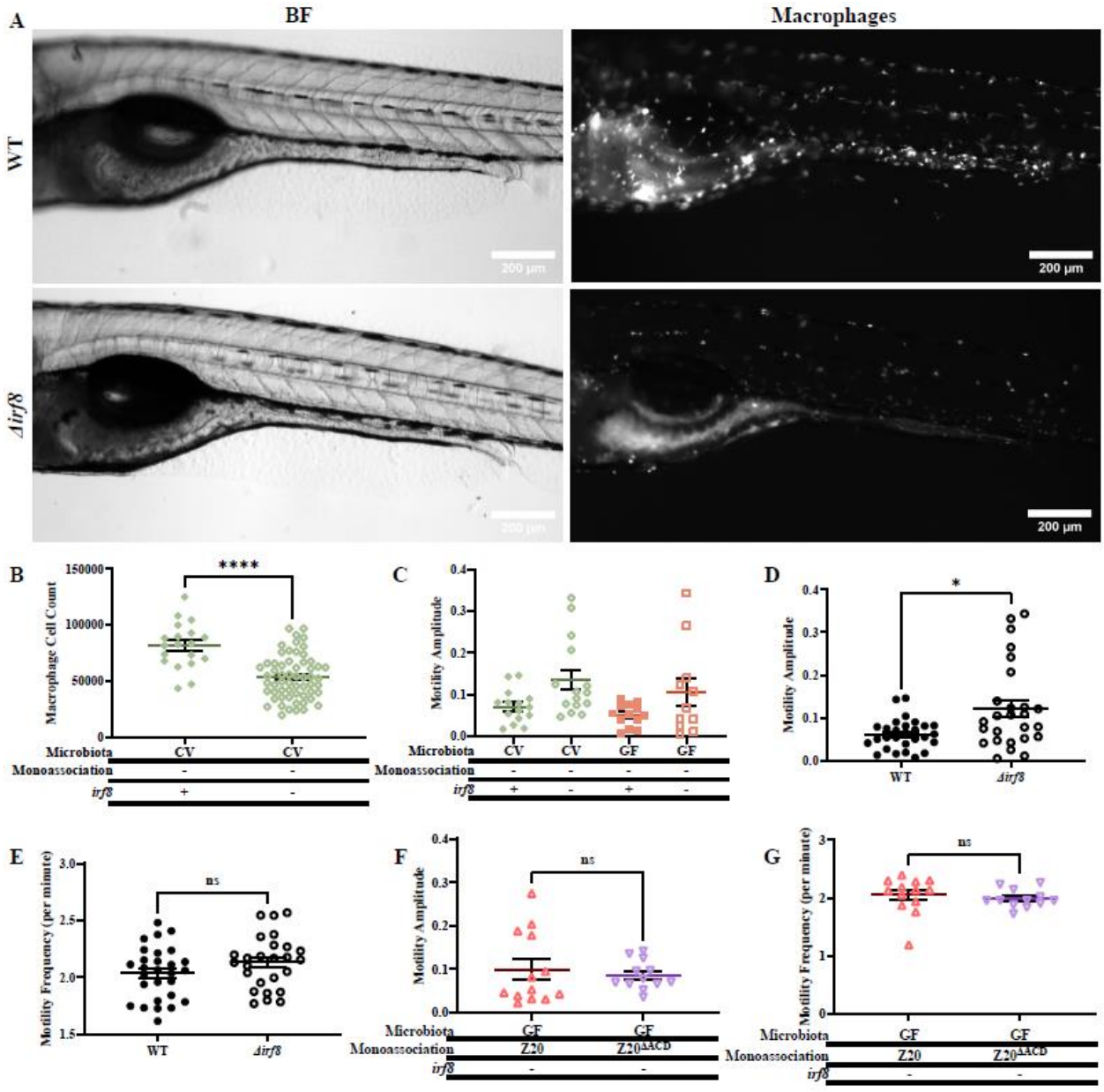

Figure 3. Macrophage Depletion Enhances Intestinal Contraction Strength. (A) Representative images captured on Nikon SMZ25 stereoscope showing conventional *tg(mpeg:mCherry)* uninjected control and *Δirf8* F0 crispants (scale bar 200 µm). (B) Macrophage cell counts of fish under conditions described in (A), counts made on whole fish in images from (A). *Δirf8* F0 crispants exhibit less macrophages compared to controls (*unpaired t test, P <0.0001*). (C) Gut motility amplitudes measured in both CV and GF fish under the same conditions as in (A), effect of microbiota not detected. (D) Gut motility amplitudes of combined data comparing WT vs *Δirf8* regardless of microbiota. *Δirf8* F0 crispants display higher gut amplitudes compared to controls (*Mann-Whitney U test, P =0.0150*). (E) Frequency of periodic gut motility under conditions outlined in (D). The distributions of gut motility frequencies are similar, with no statistically significant difference (*Mann-Whitney U test, P = 0.1306*). (F) Gut motility amplitudes for GF *Δirf8* F0 crispant fish mono-associated with either Z20 or Z20$^{\Delta ACD}$. The distributions of gut motility amplitudes are comparable, with no statistically significant difference (*unpaired t test, P = 0.5648*). (G) Frequency of periodic gut motility under the conditions described in (F). The distributions of gut motility frequencies are comparable, with no statistically significant difference (*Mann-Whitney U test, P = 0.2200*).

ACD-Mediated Activation and Recruitment of Macrophages

Previous data has demonstrated that Z20 triggers inflammation in the zebrafish intestine, primarily through the influx of neutrophils (Rolig et al., 2017). This process is contingent on signaling mediated by the proinflammatory cytokine TNFα, which Z20 has the capacity to induce in macrophages located in the vicinity of the liver in larval zebrafish (Rolig et al., 2017; Wiles et al., 2020).

To understand the role of the ACD on macrophage recruitment and activation in the intestine, *tg(TNFα:GFP);tg(mpeg:mCherry)* fish were derived GF and conventionalized or mono-associated with either Z20 or $Z20^{\Delta ACD}$. At 6 dpf and 24 hpi, their intestines were dissected for quantification of macrophages, TNFα-positive cells, and TNFα-positive macrophages (Figure 4A). The investigation revealed no significant variation in the total number of macrophages within the dissected gut across the experimental conditions (Figure 4B). This result is intriguing, particularly considering Z20's capability to trigger an influx of neutrophils into the intestine (Rolig et al., 2017). However, it is important to note that this outcome might be attributed to the study's constraint to a single time point. As neutrophils are known to dominate the initial phases of inflammation, typically arriving before macrophages (Butterfield et al., 2006). We made an intriguing discovery that the inflammatory response induced by Z20 was attributed to the ACD. Fish that were mono-associated with Z20 exhibited approximately a 100% increase in the number of TNFα-positive cells compared to those mono-associated with $Z20^{\Delta ACD}$ (Figure 4C). The most remarkable response was observed in gut-associated macrophages, which displayed a substantial difference in Z20-associated fish compared to all the other condition. In particular,

they exhibited an almost 500% increase in comparison to Z20$^{\Delta ACD}$ mono-associated fish, suggesting the ability of the ACD to target macrophages (Figure 4D).

While we did not observe an influx of macrophages in the zebrafish intestines, we remained curious about the ACD-mediated effects on the localization of macrophages. Considering the tissue damage that was evident in Figure 1A, particularly in the vent of the larval zebrafish, we employed live zebrafish for an in-depth exploration. *Tg(mpeg:mCherry)* fish were derived GF and conventionalized or mono-associated with either Z20 or Z20$^{\Delta ACD}$.

Following 24 hours of bacterial association, on 6 dpf, live fish were imaged using a stereomicroscope (Figure 4E). These images clearly revealed an influx of macrophages near the vent of fish mono-associated with Z20, a phenomenon not observed in any other fish conditions (Figure 4E). A quantitative analysis of these images pinpointed a peak in macrophage intensity at approximately 1500 μm, which corresponded to the vent location in Z20-associated fish (Figure 4F). Remarkably, GF and Z20$^{\Delta ACD}$-associated fish exhibited macrophage intensity profiles more similar to each other than any other condition (Figure 4F). This similarity could be attributed to the fact that having a single non-pathogenic microbe present in the intestine is more representative of a GF environment than a CVZ state. This further underscores the impact of the ACD, as Z20 and Z20$^{\Delta ACD}$ differ only by the deletion of a protein domain, highlighting the pivotal role the ACD plays in immune cell activation.

These results collectively highlight the ACD-mediated activation and recruitment of macrophages within the larval zebrafish gut, providing insights into the host response to pathogenic challenges.

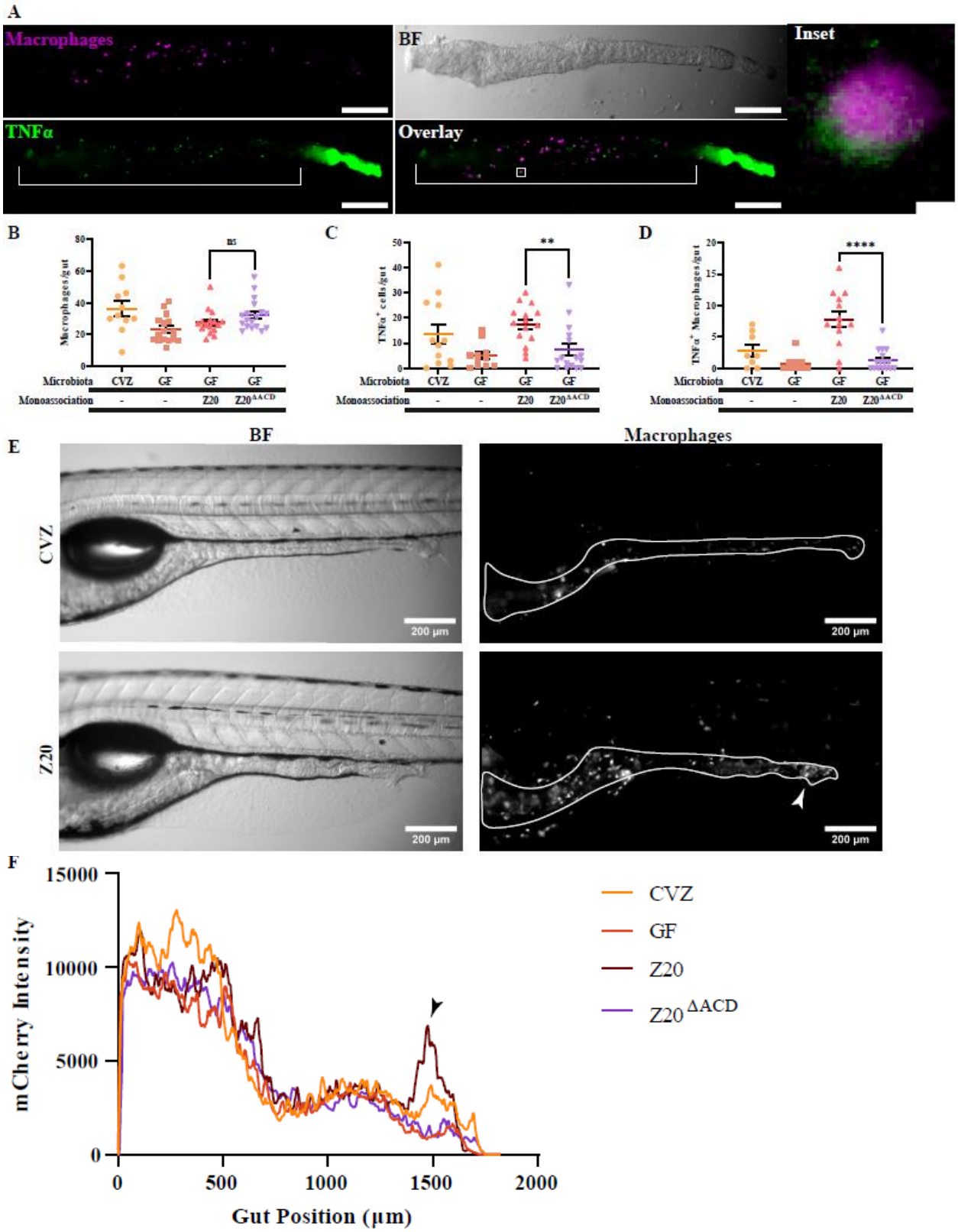
A
Macrophages
BF
Inset
TNFα
Overlay
B
Macrophages/gut
ns
C
TNFα+ cells/gut
**
D
TNFα+ Macrophages/gut
****
Microbiota
CVZ
GF
GF
GF
Monoassociation
-
-
Z20
Z20ΔACD
E
BF
Macrophages
CVZ
Z20
200 µm
F
mCherry Intensity
Gut Position (µm)
CVZ
GF
Z20
Z20 ΔACD

Figure 4. ACD-mediated Activation and Recruitment of Macrophages. (A) Representative images of dissected guts from 6 dpf *tg(TNFα:GFP);tg(mpeg:mCherry)* GF larval zebrafish mono-associated with Z20. Images were captured using a Leica stereoscope (scale bar 200 μm). The inset highlights a TNFα-positive macrophage (scale bar 5 μm). (B) Quantification of macrophage cell numbers per dissected gut in GF fish that were either conventionalized or mono-associated with Z20 or $Z20^{\Delta ACD}$. Dissected guts show no difference in the number of macrophages across all conditions (*unpaired t-test, P = 0.1465*) (C) Enumeration of TNFα-positive cells per dissected gut within the countable region (anterior of the gut, outside of the TNFα posterior GFP expression, indicated by the white bracket in (A)) in fish under the same conditions as in (B). Dissected guts of fish monoassociated with Z20 show more TNFα-positive cells (*unpaired t-test, P = 0.003*). (D) Calculation of the number of the TNFα-positive macrophages per dissected gut counted in the same region as described in (C), for fish under the same conditions as in (B). Dissected guts of fish mono-associated with Z20 show more TNFα-positive macrophages (*unpaired t-test, P < 0.001*). (E) Representative images of *tg(mpeg:mCherry)* GF fish either conventionalized or mono-associated with Z20 (scale bar 200 μm). (F) 1D mCherry Intensity profiles along the intestine of fish under the same conditions as described in (B). Each line represents the average of mCherry intensity across fish for each condition. Designated region of interest for the area measured outlined in white on the mCherry images in (E). Live fish mono-associated with Z20 show an influx of macrophages at the vent, black arrowhead and white arrowhead indicate macrophage influx on both the image and the graph.

Z20-Mediated Cell Death in Live Larval Zebrafish

Z20's ability to trigger an inflammatory response in macrophages in an ACD-dependent manner, coupled with the substantial tissue damage observed in the intestine, lent weight to the hypothesis that macrophages could be the primary targets of the ACD in a host organism (Figures 1 and 4) (Ma et al., 2009). To understand the role of Z20 in macrophage death in a live organism, *tg(mpeg:mCherry)* fish were derived GF and conventionalized or mono-associated with Z20. At 6 dpf and 24 hpi, live fish were subjected to Acridine Orange (AO) staining, a membrane-permeable dye fluoresces within acidic lysosomal vesicles, preferentially staining apoptotic cells (Abrams et al., 1993). Focusing our attention on the vent, at the location of the macrophage influx, it became evident that fish mono-associated with Z20 exhibited more extensive AO staining the vent area in comparison to CVZ and GF fish (Figure 4F & 5A).

Our quantitative analysis revealed that fish mono-associated with Z20 exhibited higher total AO intensity compared to the other conditions (Figure 5B). To assess whether Z20 was selectively targeting macrophages, we calculated the fractional overlap of total mCherry intensity coinciding with AO intensity. This calculation indicated that fish mono-associated with Z20 had

a higher percentage overlap, suggesting that more macrophages were being affected in Z20-associated fish (Figure 5C). However, this percentage overlap was only around 10%, indicating the existence of a substantial population of macrophages that were not undergoing cell death, therefore, were not specifically being targeted (Figure 5C).

These results collectively demonstrate that Z20 induces cell death in live larval zebrafish

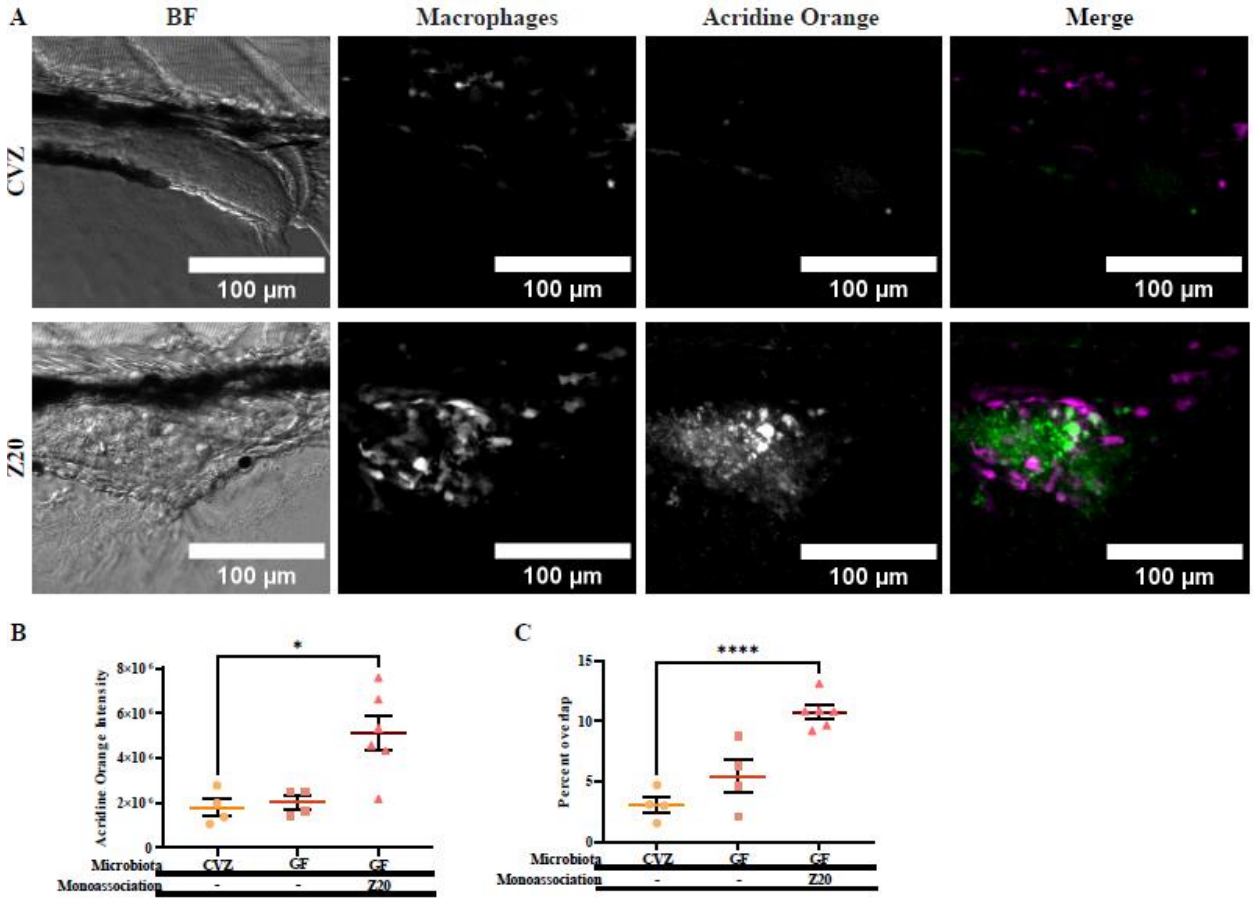

Figure 5. Z20-Mediated Cell death in Live Larval Zebrafish. (A) Representative images of vents from 6 dpf *tg(mpeg:mCherry)* GF larval zebrafish that were conventionalized or mono-associated with Z20. Live fish were stained with Acridine Orange to visualize cell death (scale bar 100 µm). (B) Quantification of total Acridine Orange intensity in the vent region of fish under the same conditions as described in (A). Fish mono-associated with Z20 show more Acridine Orange stain (*unpaired t-test, P = 0.0113*). (D) Calculation of the percentage overlap of total mCherry intensity that coincides with the total Acridine Orange intensity in the vent region of fish under the same condtions as described in (A). Fish mono-associated with Z20 show more percent overlap (*unpaired t-test, P < 0.0001*).

but does not exhibit specific targeting of macrophages, as evidenced by changes in AO intensity and the observed percentage overlap.

Z20-Mediated Macrophage Redistribution

While macrophages were not the sole target of the ACD, the abrupt accumulation of macrophages at the vent of larval zebrafish raised questions about the dynamics and timing of this influx, and our custom-built light sheet microscope provided the means to investigate this further.

Light sheet fluorescence microscopy offers rapid imaging of the entire zebrafish intestine in two channels in approximately 90 seconds, providing the necessary speed to capture clear images of these motile immune cells while outpacing the blurring effects induced by peristalsis (Jemielita et al., 2014). We conducted experiments with *tg(mpeg:mCherry)* fish mono-associated with Z20, and observed them from 13 hpi to 26 hpi (Figure 6A). We observe, as expected, an accumulation of macrophages at the vent region. In addition, quantification of macrophage positions in six separate fish shows a shifting macrophage distribution. Kernel Density Estimate plots, essentially smoothed histograms of cellular positions, reveal a decrease in macrophage density within the midgut over time, in contrast to the notable increase in macrophage density in the vent region (Figure 6C). Together, this data serves as strong evidence that in the context of Z20 mono-association, macrophages primarily relocate from the midgut to the vent.

Notably, the total macrophage count remained relatively stable over time (Figure 6D). While there was a minor decline of approximately 10% throughout the 13-hour observation period, this reduction could be attributed to the macrophage deaths associated with Z20, as observed in Figure 5, or potentially be due to photobleaching.

The results presented in this study provide valuable insights into the ACD-mediated effects on tissue damage, intestinal motility, competitive interactions, and host immune

responses in larval zebrafish. Notably, our findings demonstrate that the zebrafish-isolate Z20 can induce substantial tissue damage and inflammation in the zebrafish intestine, even in the absence of the cholerae toxin, within a relatively short period of 13 hours. This research contributes to our understanding of the intricate interplay between a bacterium like Z20 and the host's immune response, providing essential information on the role of the ACD in shaping these interaction.

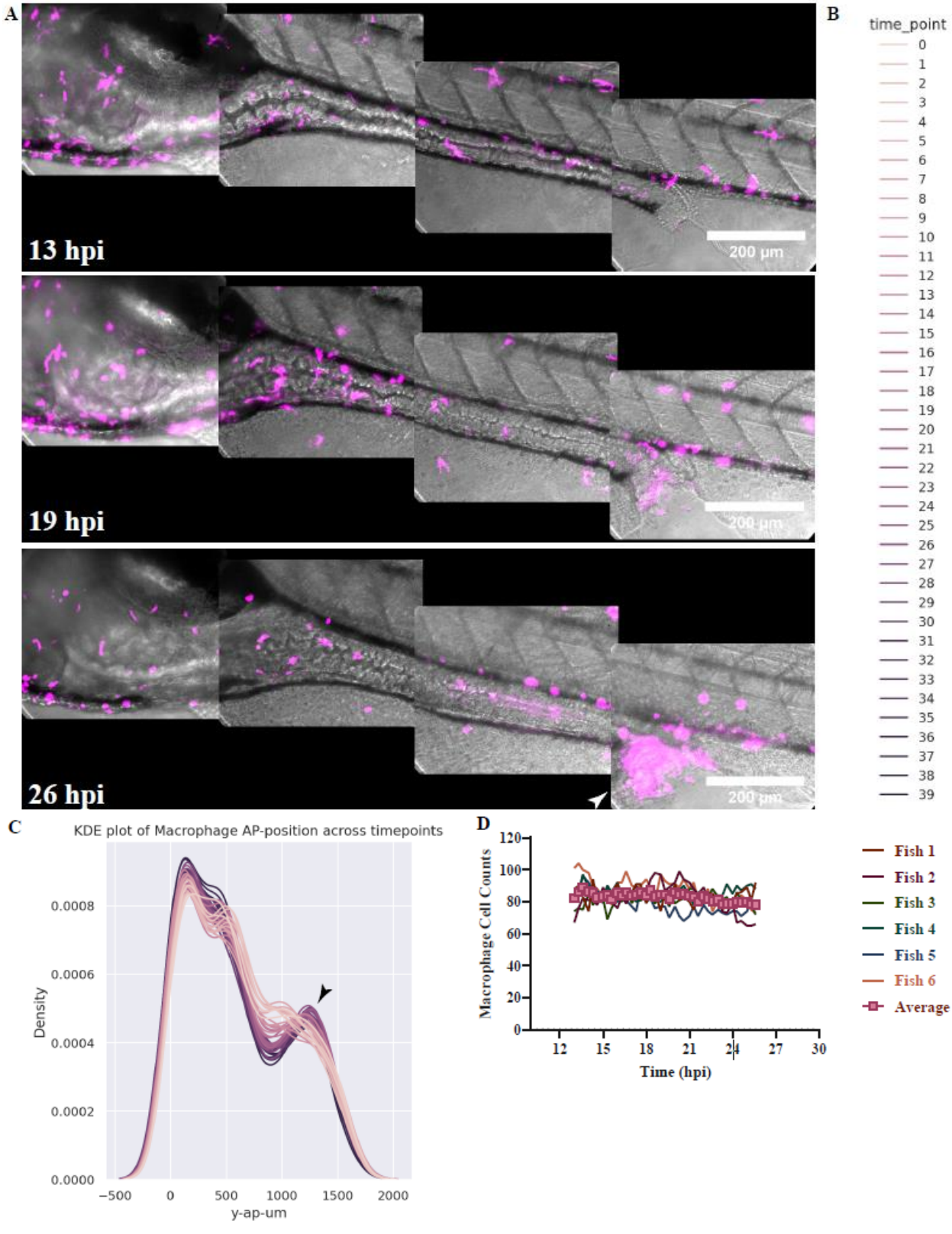
A
13 hpi
19 hpi
26 hpi
200 µm
B
time_point
0
1
2
3
4
5
6
7
8
9
10
11
12
13
14
15
16
17
18
19
20
21
22
23
24
25
26
27
28
29
30
31
32
33
34
35
36
37
38
39
C
KDE plot of Macrophage AP-position across timepoints
Density
0.0000
0.0002
0.0004
0.0006
0.0008
−500
0
500
1000
1500
2000
y-ap-um
D
Macrophage Cell Counts
0
20
40
60
80
100
120
12
15
18
21
24
27
30
Time (hpi)
Fish 1
Fish 2
Fish 3
Fish 4
Fish 5
Fish 6
Average

Figure 6. Macrophage Redistribution. (A) Representative merged images of GF *tg(mpeg:mCherry)* fish mono-associated with Z20 from 13 to 26 hpi. Images include a BF channel and an mCherry-labelled macropahge channel shown in magenta (scale bar 200 μm). (B) Legend of time point scale for fish imaged in (A) for plot in (C). Initial time pont 0 refers to 13 hpi, with an image taken every 20 minutes after that. Time points range from light to dark from 0 to 39. (C) Kernel Density Estimate (KDE) plot illustrating the density of the mCherry intensity along the anterior-posterior axis of the gut overtime. Plot shows data of macrophage density changing overtime, each line is data average from 6 fish. The vent, the area of macrophage influx, is indicated with a white arrow head on the overlayed image, and a black arrow head on the KDE plot. (D) Macrophage cell counts in the whole gut of the zebrafish overtime. Counts for 6 individual fish plotted with the average plotted with pink squares. The macrophage number remians flat overtime, showing a slight decline with a regression line slope of -6.9 +/- 1.1 macrophages per hour.

Discussion

The findings of our study reveal how the *Vibrio* T6SS causes intestinal tissue damage through the ACD of its VgrG-1 tip protein and shed light on how this tissue damage leads to increased intestinal motility. Our initial hypothesis about the mechanism behind ACD-mediated changes in intestinal motility posited that the ACD was directly responsible for macrophage death. Instead, our results revealed that ACD-induced tissue damage in the posterior gut redistributed macrophages away from their even distribution along the length of the intestine. The effect of this redistribution recapitulated intestine-wide depletion of macrophages by CRISPR-mediated mutagenesis of the *irf8* locus. These results reveal the complex and indirect effects of *Vibrio*'s eukaryotic-targeting T6SS ACD and have important implications for understanding the impacts of *Vibrio* infection on intestinal physiology beyond those described for cholerae toxin.

One key observation from our studies is that the ACD of Z20 did not lead to widespread macrophage death, as we had initially anticipated based on *in vitro* data involving *Vibrio cholerae* (Ma et al., 2009). Instead, we observed that despite extensive ACD-associated cell death in the distal intestine, most of macrophages in this region were not stained with Acridine Orange, indicating their viability. A strength of our zebrafish model is the ability to perform live

imaging on the entire length of the intestine and monitor the complete population of intestinal macrophages. From this analysis we found that the total population size of intestinal macrophages was stable over the course of the *Vibrio* infection, but the spatial distribution changed dramatically, leaving a region in the mid to distal region largely denuded of macrophages which normally reside in high density and in close proximity to enteric neurons. This apparent contradiction highlights the importance of studying these interactions in a live organism, as the complexity of the *in vivo* environment can lead to unexpected outcomes. Utilizing a custom-built light sheet microscope and the zebrafish model allowed us to gain unique insights into the intricacies of macrophage redistribution over time. Nevertheless, it is essential to acknowledge that our experimental setup, involving specimen embedded in 1% agarose, limits the natural swimming behavior of the fish and makes our findings specific to the laboratory setting.

Recent studies have started to uncover the role of macrophage-enteric neuron interactions in regulating intestinal motility. In the mouse model, muscularis macrophages activate enteric neurons via BMP2 signaling, while enteric neurons modulate muscularis macrophage production through CSF1 signaling (Muller et al., 2014). In zebrafish, the muscularis macrophages are closely associated with neural processes, spanning multiple layers of the gut wall and play a crucial role in intestinal motility in larvae (Graves et al., 2021). Additionally, these macrophages contribute to gut motility regulation by producing C1q (Pendse et al., 2023). Our study highlights that the ACD-mediated increase in contractility of the zebrafish intestine is contingent upon the relocation of macrophages in larval zebrafish. This phenomenon implies that the macrophage redistribution from the mid-gut to the distal gut disrupts the macrophage-enteric

neuron communication, ultimately affecting intestinal motility. A host-microbe phenomenon involving recruitment of tissue resident macrophages impeding their regular functions is not uncommon in zebrafish. For instance, *Mycobateria marinum* has been shown to recruit macrophages to infection sites, redirecting their developmental program of migrating to the optic tectum to differentiate into microglia (Davis et al., 2002). Similarly, in the case of our zebrafish muscularis macrophages, their recruitment to the vent by the *Vibrio* ACD appears to hinder their normal function of communicating with the enteric neurons to regulate intestinal motility.

Building on this foundation, further investigations into the Z20-mediated redistribution of macrophages over time and its relationship with enteric neurons in live larval zebrafish could yield valuable insights into the intricate crosstalk between these cell types. This knowledge could open new avenues for exploring the role of immune cells and their interactions with the enteric nervous system in maintaining intestinal homeostasis and motility.

In conclusion, our research highlights the complexity of host-pathogen interactions and emphasizes the importance of studying these processes *in vivo*. While our findings challenge conventional wisdom, they pave the way for more nuanced investigations into the mechanisms underlying *Vibrio* pathogenesis and its impact on intestinal motility.

Methods

Ethics Statement

All experiments involving zebrafish followed approved protocols set by the University of Oregon Institutional Animal Care and Use Committee and adhered to standard methods (Westerfield, 2000).

Gnotobiotic Techniques

Wild-type AB, *tg(mpeg:mCherry)*, or *tg(tnfα:GFP);tg(mpeg:mCherry)* zebrafish were derived germ-free (GF) and subsequently colonized with bacterial strains, following established protocols (Melancon et al., 2017). In brief, fertilized eggs were collected and incubated in sterile embryo media (EM) containing 100 μg/mL ampicillin, 10 μg/mL gentamycin, 1 μg/mL tetracycline, 1 μg/mL chloramphenicol, and 250 ng/mL amphotericin B for approximately 6 hours. Following this incubation period, embryos were thoroughly rinsed first in sterile EM containing 0.003% sodium hypochlorite and then in sterile EM containing 0.1% polyvinylpyrrolidone-iodine. These sterilized embryos were then distributed into T25 tissue culture flasks, with a density of one embryo per mL in 15 mL of sterile EM. Notably, during the experiments, the embryos relied on yolk-derived nutrients and were not provided with external feeding. The sterility of the flasks containing larval zebrafish was inspected prior to the experiments.

Bacterial Strains

Aeromonas (ZOR0001, PRJNA205571) and *Vibrio* (ZWU0020, PRJNA205585) were isolated from the zebrafish intestinal tract as previously described. To prepare the bacterial strains for colonization at specific time points, both the *Aeromonas* and *Vibrio* cultures were first grown overnight in Luria Broth (LB) under agitation at a temperature of 30ºC. Then, bacterial cultures were pelleted through centrifugation for a duration of 3 minutes at 7,000 x g, followed by two rounds of washing in sterile EM. An inoculum of 10^6 colony-forming unit per milliliter (CFU/mL) was consistently employed across all experiments for both the *Aeromonas* and *Vibrio* strains, with this inoculum directly introduced to the flask water.

Molecular and Genetic Manipulation

Unless otherwise specified, standard molecular techniques were employed in our experiments. Reagents were used in accordance with the manufacturer's instructions. We used restriction enzymes and various other molecular biology reagents for tasks such as polymerase chain reaction (PCR) and nucleic acid modifications. The reagents were primarily obtained from New England BioLabs. To purify plasmids and PCR amplicons, we used kits from Zymo Research. DNA oligonucleotides were synthesized by Integrated DNA Technologies. The sequencing of cloned genes was verified by Sanger sequencing, conducted by Sequetech. A Leica MZ10 F fluorescence stereomicroscope, equipped with a 1x objective lens, was used for the screening of fluorescent bacterial colonies. Genome and gene sequences were retrieved from "The Integrated Microbial Genomes & Microbiome Samples" (IMG/M) website (Chen et al., 2017).

Construction of Gene Deletion

The construction of a markerless, in-frame deletion was accomplished using allelic exchange and the pAX2 allelic exchange vector as previously described (Wiles et al., 2018). Specifically, the generation of $Z20^{\Delta ACD}$ via deletion of ACD was achieved by initially constructing an *ACD* allelic exchange cassette. This cassette was created through splice by overlap extension (SOE) PCR and was designed to fuse the beginning codon and ending codon of the actin crosslinking domain of the VgrG-1 protein. Two pairs of PCR primer were designed to amplify the 5' and 3' homology regions flanking the ACD respectively from the *Vibrio* ZWU0020 genomic DNA. The primer pairs were as follows: 5'-CCCAATGATAGCCACGGTTG-3' + 5'-CCATTCCATTTTCCACTAGGCTAAAGGACACACCTT-3' and 5'-AAGGTGTGTCCTTTAGCCTAGTGGAAAATGGAATGG-3' + 5'-

GGCGCAAGATTTTCAATCA-3’. The resulting amplicons from the 5’ and 3’ regions were spliced together, and the SOE product was ligated into a pAX2-based allelic exchange vector, resulting in the pAX2-ZWU0020-ACD vector.

The pAX2-ZWU0020-ACD vector was introduced into *Vibrio* via a conjugation process utilizing *E.coli* SM10 as a donor strain as previously described (Wiles et al., 2018). Briefly, *Vibrio* and SM10/pAX2-ZWU0020-ACD were mixed 1:1 on a filter disk and placed on tryptic soy agar (TSA). The mating mixture was then incubated at 30ºC overnight. After the incubation period, bacteria were recovered and spread onto TSA containing gentamicin. These plates were incubated overnight at 37ºC to select for *Vibrio* merodiploids. Isolated merodiploid colonies were screened for successful deletion of the ACD. Putative mutants were genotyped though PCR with primers flanking *VgrG-1* locus. This genotyping produced two differently sized amplicons, representing the wild-type and mutant alleles. The primers used for genotyping were as follows: 5’-CGGAGCTTTGGTCAATCTCA-3’ + 5’-AGGTCTCTCCGTGGAAAACA-3’

The mutated strain did not exhibit any discernable fitness defects *in vivo* as measured by the ability to colonize the zebrafish gut (Figure 2E).

Culture-Based Quantification of Bacterial Population

The dissection of larval guts were executed in accordance with established procedures (Milligan-Myhre et al., 2011). Then, the dissected guts were carefully harvested and transferred to 1.5 mL tubes, each containing sterile 0.7% saline and approximately 100 μL of 0.5 mm zirconium oxide beads. To facilitate homogenization, a bullet blender tissue homogenizer was used, with the guts undergoing homogenization for a duration of 30 seconds at power level 4. Following homogenization, lysates were serially plated on LB agar plates and incubated overnight at a

temperature of 30ºC for an enumeration of CFU to determine bacterial load as previously described (Logan et al., 2018; Wiles et al., 2016).

Measuring Intestinal Motility

Intestinal motility in larval zebrafish was assessed using Differential Interference Contrast (DIC) microscopy and image velocimetry as previously described (Baker et al., 2015). DIC videos were recorded at 5 frames per second for five minutes in the distal end of the intestine, outlined in Figure $2A_1$. For analysis, we employed open-source particle image velocimetry (PIV) software (Thielicke & Stamhuis, 2014) to calculate a velocity vector field from frame to frame in the time-series, and then characterized the frequency and amplitudes of gut motions along the anterior-posterior (AP) axis using custom software previously described (Ganz et al., 2018). We focus on the AP component of the vector field, averaging it along the dorsal-ventral direction to obtain a scalar velocity measure at each position along the gut axis and each time point. The frequency of gut contractions was determined by identifying the location of the first peak in the temporal autocorrelation of motility, while the amplitude of contractions was calculated as the square root of the spatially averaged power spectrum at the previously determined frequency, providing a quantitative measure of the magnitude of periodic gut motion.

Light Sheet Fluorescence Microscopy

The overnight imaging of macrophage displacement was conducted using a custom-built light sheet fluorescence microscope, based on a previously described design (Keller et al., 2008), and described in detail elsewhere (Jemielita et al., 2014; Taormina et al., 2012). In brief, this imaging system involves the rapid scanning of a laser beam using a galvanometer mirror, followed by demagnification to create a thin sheet of excitation light. Positioned perpendicular to this sheet,

an objective lens captures the fluorescence emission within the optical section. The sample is then scanned along the detection coordinate, enabling the generation of a three-dimensional image. To image the entire extent of the intestine, which measures approximately 1200x300x150 microns), we sequentially image four sub-regions and computationally register the images after acquisition. Unless otherwise specified in the text, all exposure times are 33 ms with an excitation laser power of 5 mW. For all light sheet imaging, a 5.5 megapixel sCMOS camera was used, in conjunction with a 40x 1.0NA objective lens. For time series imaging, scans occurred at 20 minute intervals for 12 hour durations.

Sample Handling and Mounting for Imaging Experiments

Sample mounting was done following previously established protocols (Jemielita et al., 2014). Larval 6dpf zebrafish were carefully removed from the culture flask. To facilitate anesthesia, specimen were immersed in sterile EM containing 120 μg/mL tricaine methanesulfonate.

Mounting for Light Sheet Imaging

Each anesthetized specimen was briefly immersed in low melt agarose with a concentration ranging from 0.7-1% and drawn into a glass capillary, which was then mounted onto a sample holder. The maximum temperature of the agarose did not exceed 42 ºC to ensure the well-being of the specimens. The agar-embedded specimens were partially extruded from the capillary to ensure that the excitation and emission optical paths did not traverse glass interfaces which could introduce unwanted artifacts during imaging. The specimen holder had the capacity to hold up to six samples simultaneously, all of which are immersed in sterile EM maintained at a temperature of 28ºC. All long-term imaging experiments were conducted overnight, typically beginning in the late afternoon.

Mounting for Confocal Imaging

Each anesthetized specimen was briefly immersed in 1% low melt agarose and carefully transferred to a depression microscope slide with enough agar to embed the specimen. The agar-embedded specimens were then covered with water for imaging with a Leica SPE confocal microscope equipped with a 40x 0.80NA water immersion lens.

Mounting for Stereoscope Imaging

Each anesthetized specimen was carefully embedded in 4% methylcellulose on a microscope slide. For imaging, two types of stereomicroscopes were used, a Leica MZ10 F fluorescence stereomicroscope, equipped with a 1x, 1.6x and 2.0x objective lens and Leica DFC365 FX camera or a Nikon SMZ25 stereomicroscope.

Irf8 sgRNA Cas9 injections

All sgRNAs used were previously designed and characterized with a 100% success rate (Keatinge et al., 2021). sgRNAs used are as follows: 5'-ATAAAGCTGAACCAGCGACATGG3') and (5' TGGTGAGCAGTCCATGTCAGTGG-3'. The RNA oligonucleotides were resuspended to 20 μM with nuclease free water and stored at -20ºC until use. For *in vivo* applications, 1 nL of an injection mixture composed of 1μL of each sgRNA, 1μL of Cas9, 1μL of Phenol Red (0.125%) were injected into the yolk at the one-cell stage. Phenol Red was used to screen for injected developing embryos during the GF derivation process.

TNFα and Macrophage Quantification from Dissected Intestines

Tg(tnfα:GFP);tg(mpeg:mCherry) larval zebrafish were mounted for stereoscope imaging, their intestines were dissected, and imaged using the Leica MZ10 F fluorescence stereomicroscope,

equipped with a 1x, 1.6x and 2.0x objective lens and Leica DFC365 FX camera. The number of GFP positive, mCherry positive, and double positive cells were quantified visually using ImageJ.

Macrophage Image Analysis

Macrophages distributions were assessed from fluorescence stereomicroscope images using custom code. First, a region of interest (ROI) corresponding to the intestine was manually outlined. Pixels with mCherry intensity above a threshold background value were identified and summed along the dorsal-ventral axis to provide a measure of macrophage density along the gut's anterior-to-posterior axis.

Macrophages were identified from three-dimensional light sheet fluorescence microscopy images by median filtering followed by thresholding and segmentation to identify contiguous pixels.

Acridine Orange Staining in Live Larval Zebrafish

To visualize apoptosis in live larval zebrafish, the Acridine Orange dye was used (Elmore, 2007). The analysis of apoptosis was conducted in 6 days post fertilization (dpf) larval zebrafish that were derived GF then conventionalized or mono-associated with Z20 or Z20$^{\Delta ACD}$. The larvae were anesthetized then immersed in sterile EM containing 0.3125 μg/mL Acridine Orange for a duration of 10 minutes in the dark. Following the staining, the larvae were washed in sterile EM three times to remove excess dye. Specimens were then mounted for imaging on the Leica SPE confocal equipped with a 40x water immersion lens.

Data and Statistical Analysis

Data analysis and visualization were conducted using GraphPad Prism software. Means and standard error of the mean (SEM) were plotted. Specific details about the statistical tests

conducted for each dataset can be found in the respective figure legends. In all analyses, a significance level of $P \leq 0.05$ was adopted.

CHAPTER III

CONCLUDING REMARKS

Our dissection of the molecular, cellular, and organismal impacts of the *Vibrio* T6SS ACD, uncovered layers of complexity in the regulation of gut motility in larval zebrafish. This exploration revealed how the local consequences of bacterial infection, such as tissue damage and cell death, can redistribute tissue resident macrophages from other organ regions, ultimately impacting the delicate balance of the host's intestinal motility.

Based on previous studies of *V. cholerae's* T6SS ACD toxicity in cultured macrophages, we started the project with the hypothesis that ACD killing of macrophages would be responsible for gut motility changes attributed to this domain. Use of the zebrafish model and our custom-built light sheet microscope allowed us to witness the impacts of Vibrio's T6SS ACD in living animals across the entire length of their intestines. We observed only limited macrophage killing, but instead documented the migration of macrophages from midgut to the distal vent region where *Vibrio* caused widespread tissue damage in an ACD-dependent manner. The data collected in our study suggests that *Vibrio* impacts on the zebrafish host are mediated both by direct contact with the intestinal epithelium and through in direct effects of the damage it causes, by redirecting tissue-resident macrophages away from their normal regulatory interactions with enteric neurons. The consequence is more powerful and more variable gut contractions.

To comprehend the full implications of these findings, future research should delve into the cellular interactions between the T6SS and host target cell types. Our experimental set up presents an opportunity for researchers to explore the dynamics of these interactions by combining fluorescently tagged bacteria with zebrafish expressing fluorescently labeled cell

types. This approach can help elucidate the precise cell types targeted by *Vibrio* species to trigger the redistribution of macrophages. Among these potential target cells are microbe-sensing enteroendocrine cells that synapse with enteric neurons, and mucin-secreting goblet cells that would be the source of T6SS-stimulated mucin production in zebrafish (Breen et al., 2021; Yu et al., 2020). Future researchers should also explore whether this T6SS-dependent increase in mucin production is ACD-mediated.

Our finding of the ACD-dependent redistribution of macrophages resulting in increased intestinal contractions raises the possibility of other ACD-dependent impacts on intestinal pathology mediated through indirect effects on the enteric nervous system. Research from our group has shown that the enteric nervous system is required for intestinal barrier function and tight junction integrity (Hamilton et al., 2022). It is possible that indirect effects of the ACD on enteric neurons could exacerbate intestinal inflammation caused by increased intestinal permeability, allowing LPS dissemination from the lumen which would increase proinflammatory cytokines such as TNFα (Cani et al., 2008; Ha et al., 2014).

Our studies lay the groundwork for future investigations into the complex relationship between macrophages and enteric neurons. Employing our model system, future investigations can delve into the effects of the ACD on BMP2, CSF1, and Cq1 signaling in live fish, potentially charting unexplored territories of this multifaceted interplay (Earley et al., 2018; Muller et al., 2014; Pendse et al., 2023). The zebrafish model holds great promise for a more complete comprehension of the microbial factors that can modulate gut motility and their implications for host health.

RERENCES CITED

Abrams, J. M., White, K., Fessler, L. I., & Steller, H. (1993). Programmed cell death during Drosophila embryogenesis. *Development*, *117*(1), 29–43. https://doi.org/10.1242/dev.117.1.29

Baker, R. P., Taormina, M. J., Jemielita, M., & Parthasarathy, R. (2015). A combined light sheet fluorescence and differential interference contrast microscope for live imaging of multicellular specimens. *Journal of Microscopy*, *258*(2), 105–112. https://doi.org/10.1111/jmi.12220

Basler, M., Ho, B. T., & Mekalanos, J. J. (2013). Tit-for-Tat: Type VI Secretion System Counterattack during Bacterial Cell-Cell Interactions. *Cell*, *152*(4), 884–894. https://doi.org/10.1016/j.cell.2013.01.042

Bill, B. R., Petzold, A. M., Clark, K. J., Schimmenti, L. A., & Ekker, S. C. (2009). A Primer for Morpholino Use in Zebrafish. *Zebrafish*, *6*(1), 69–77. https://doi.org/10.1089/zeb.2008.0555

Breen, P., Winters, A. D., Theis, K. R., & Withey, J. H. (2021). The Vibrio cholerae Type Six Secretion System Is Dispensable for Colonization but Affects Pathogenesis and the Structure of Zebrafish Intestinal Microbiome. *Infection and Immunity*, *89*(9). https://doi.org/10.1128/iai.00151-21

Brooks, T. M., Unterweger, D., Bachmann, V., Kostiuk, B., & Pukatzki, S. (2013). Lytic Activity of the Vibrio cholerae Type VI Secretion Toxin VgrG-3 Is Inhibited by the Antitoxin TsaB. *The Journal of Biological Chemistry*, *288*(11), 7618–7625. https://doi.org/10.1074/jbc.M112.436725

Brown, A. J., Goldsworthy, S. M., Barnes, A. A., Eilert, M. M., Tcheang, L., Daniels, D., Muir, A. I., Wigglesworth, M. J., Kinghorn, I., Fraser, N. J., Pike, N. B., Strum, J. C., Steplewski, K. M., Murdock, P. R., Holder, J. C., Marshall, F. H., Szekeres, P. G., Wilson, S., Ignar, D. M., … Dowell, S. J. (2003). The Orphan G Protein-coupled Receptors GPR41 and GPR43 Are Activated by Propionate and Other Short Chain Carboxylic Acids *. *Journal of Biological Chemistry*, *278*(13), 11312–11319. https://doi.org/10.1074/jbc.M211609200

Butterfield, T. A., Best, T. M., & Merrick, M. A. (2006). The Dual Roles of Neutrophils and Macrophages in Inflammation: A Critical Balance Between Tissue Damage and Repair. *Journal of Athletic Training*, *41*(4), 457–465.

Cani, P. D., Bibiloni, R., Knauf, C., Waget, A., Neyrinck, A. M., Delzenne, N. M., & Burcelin, R. (2008). Changes in Gut Microbiota Control Metabolic Endotoxemia-Induced Inflammation in High-Fat Diet–Induced Obesity and Diabetes in Mice. *Diabetes*, *57*(6), 1470–1481. https://doi.org/10.2337/db07-1403

Carvalho, F. A., Koren, O., Goodrich, J. K., Johansson, M. E. V., Nalbantoglu, I., Aitken, J. D., Su, Y., Chassaing, B., Walters, W. A., González, A., Clemente, J. C., Cullender, T. C., Barnich, N., Darfeuille-Michaud, A., Vijay-Kumar, M., Knight, R., Ley, R. E., & Gewirtz, A. T. (2012). Transient inability to manage proteobacteria promotes chronic gut inflammation in TLR5-deficient mice. *Cell Host & Microbe*, *12*(2), 139–152. https://doi.org/10.1016/j.chom.2012.07.004

Cascales, E. (2008). The type VI secretion toolkit. *EMBO Reports*, *9*(8), 735–741. https://doi.org/10.1038/embor.2008.131

Chatterjee, S., Ghosh, K., Raychoudhuri, A., Chowdhury, G., Bhattacharya, M. K., Mukhopadhyay, A. K., Ramamurthy, T., Bhattacharya, S. K., Klose, K. E., & Nandy, R. K. (2009). Incidence, Virulence Factors, and Clonality among Clinical Strains of Non-O1, Non-O139 Vibrio cholerae Isolates from Hospitalized Diarrheal Patients in Kolkata, India. *Journal of Clinical Microbiology*, *47*(4), 1087–1095. https://doi.org/10.1128/jcm.02026-08

Chen, I.-M. A., Markowitz, V. M., Chu, K., Palaniappan, K., Szeto, E., Pillay, M., Ratner, A., Huang, J., Andersen, E., Huntemann, M., Varghese, N., Hadjithomas, M., Tennessen, K., Nielsen, T., Ivanova, N. N., & Kyrpides, N. C. (2017). IMG/M: Integrated genome and metagenome comparative data analysis system. *Nucleic Acids Research*, *45*(D1), D507–D516. https://doi.org/10.1093/nar/gkw929

Cherrak, Y., Flaugnatti, N., Durand, E., Journet, L., & Cascales, E. (2019). Structure and Activity of the Type VI Secretion System. *Microbiology Spectrum*, *7*(4), 10.1128/microbiolspec.psib-0031–2019. https://doi.org/10.1128/microbiolspec.psib-0031-2019

Chowdhury, G., Joshi, S., Bhattacharya, S., Sekar, U., Birajdar, B., Bhattacharyya, A., Shinoda, S., & Ramamurthy, T. (2016). Extraintestinal Infections Caused by Non-toxigenic Vibrio cholerae non-O1/non-O139. *Frontiers in Microbiology*, *7*. https://www.frontiersin.org/articles/10.3389/fmicb.2016.00144

Clemens, J. D., Nair, G. B., Ahmed, T., Qadri, F., & Holmgren, J. (2017). Cholera. *The Lancet*, *390*(10101), 1539–1549. https://doi.org/10.1016/S0140-6736(17)30559-7

Davis, J. M., Clay, H., Lewis, J. L., Ghori, N., Herbomel, P., & Ramakrishnan, L. (2002). Real-Time Visualization of Mycobacterium-Macrophage Interactions Leading to Initiation of Granuloma Formation in Zebrafish Embryos. *Immunity*, *17*(6), 693–702. https://doi.org/10.1016/S1074-7613(02)00475-2

Durand, E., Derrez, E., Audoly, G., Spinelli, S., Ortiz-Lombardia, M., Raoult, D., Cascales, E., & Cambillau, C. (2012). Crystal Structure of the VgrG1 Actin Cross-linking Domain of the Vibrio cholerae Type VI Secretion System. *Journal of Biological Chemistry*, *287*(45), 38190–38199. https://doi.org/10.1074/jbc.M112.390153

Earley, A. M., Graves, C. L., & Shiau, C. E. (2018). Critical Role for a Subset of Intestinal Macrophages in Shaping Gut Microbiota in Adult Zebrafish. *Cell Reports*, *25*(2), 424–436. https://doi.org/10.1016/j.celrep.2018.09.025

Elmore, S. (2007). Apoptosis: A Review of Programmed Cell Death. *Toxicologic Pathology*, *35*(4), 495–516. https://doi.org/10.1080/01926230701320337

Fitch, M. D., & Fleming, S. E. (1999). Metabolism of short-chain fatty acids by rat colonic mucosa in vivo. *The American Journal of Physiology*, *277*(1), G31-40. https://doi.org/10.1152/ajpgi.1999.277.1.G31

Ganz, J., Baker, R. P., Hamilton, M. K., Melancon, E., Diba, P., Eisen, J. S., & Parthasarathy, R. (2018). Image velocimetry and spectral analysis enable quantitative characterization of larval zebrafish gut motility. *Neurogastroenterology & Motility*, *30*(9), e13351. https://doi.org/10.1111/nmo.13351

Graves, C. L., Chen, A., Kwon, V., & Shiau, C. E. (2021). Zebrafish harbor diverse intestinal macrophage populations including a subset intimately associated with enteric neural processes. *iScience*, *24*(6), 102496. https://doi.org/10.1016/j.isci.2021.102496

Green, E. R., & Mecsas, J. (2016). Bacterial Secretion Systems – An overview. *Microbiology Spectrum*, *4*(1), 10.1128/microbiolspec.VMBF-0012–2015. https://doi.org/10.1128/microbiolspec.VMBF-0012-2015

Ha, C. W., Lam, Y. Y., & Holmes, A. J. (2014). Mechanistic links between gut microbial community dynamics, microbial functions and metabolic health. *World Journal of Gastroenterology : WJG*, *20*(44), 16498–16517. https://doi.org/10.3748/wjg.v20.i44.16498

Hamilton, M. K., Wall, E. S., Robinson, C. D., Guillemin, K., & Eisen, J. S. (2022). Enteric nervous system modulation of luminal pH modifies the microbial environment to promote intestinal health. *PLOS Pathogens*, *18*(2), e1009989. https://doi.org/10.1371/journal.ppat.1009989

Hillary, V. E., & Ceasar, S. A. (2023). A Review on the Mechanism and Applications of CRISPR/Cas9/Cas12/Cas13/Cas14 Proteins Utilized for Genome Engineering. *Molecular Biotechnology*, *65*(3), 311–325. https://doi.org/10.1007/s12033-022-00567-0

Holmberg, A., Olsson, C., & Hennig, G. W. (2007). TTX-sensitive and TTX-insensitive control of spontaneous gut motility in the developing zebrafish (Danio rerio) larvae. *Journal of Experimental Biology*, *210*(6), 1084–1091. https://doi.org/10.1242/jeb.000935

Hsiao, A., & Zhu, J. (2020). Pathogenicity and virulence regulation of Vibrio cholerae at the interface of host-gut microbiome interactions. *Virulence*, *11*(1), 1582–1599. https://doi.org/10.1080/21505594.2020.1845039

Janeway, C. A. (1989). Approaching the asymptote? Evolution and revolution in immunology. *Cold Spring Harbor Symposia on Quantitative Biology*, *54 Pt 1*, 1–13. https://doi.org/10.1101/sqb.1989.054.01.003

Jemielita, M., Taormina, M. J., Burns, A. R., Hampton, J. S., Rolig, A. S., Guillemin, K., & Parthasarathy, R. (2014). Spatial and temporal features of the growth of a bacterial species colonizing the zebrafish gut. *mBio*, *5*(6), e01751-14. https://doi.org/10.1128/mBio.01751-14

Keatinge, M., Tsarouchas, T. M., Munir, T., Porter, N. J., Larraz, J., Gianni, D., Tsai, H.-H., Becker, C. G., Lyons, D. A., & Becker, T. (2021). CRISPR gRNA phenotypic screening in zebrafish reveals pro-regenerative genes in spinal cord injury. *PLOS Genetics*, *17*(4), e1009515. https://doi.org/10.1371/journal.pgen.1009515

Keller, P. J., Schmidt, A. D., Wittbrodt, J., & Stelzer, E. H. K. (2008). Reconstruction of Zebrafish Early Embryonic Development by Scanned Light Sheet Microscopy. *Science*, *322*(5904), 1065–1069. https://doi.org/10.1126/science.1162493

Kroll, F., Powell, G. T., Ghosh, M., Gestri, G., Antinucci, P., Hearn, T. J., Tunbak, H., Lim, S., Dennis, H. W., Fernandez, J. M., Whitmore, D., Dreosti, E., Wilson, S. W., Hoffman, E. J., & Rihel, J. (2021). A simple and effective F0 knockout method for rapid screening of behaviour and other complex phenotypes. *eLife*, *10*, e59683. https://doi.org/10.7554/eLife.59683

Logan, S. L., Thomas, J., Yan, J., Baker, R. P., Shields, D. S., Xavier, J. B., Hammer, B. K., & Parthasarathy, R. (2018). The *Vibrio cholerae* type VI secretion system can modulate host intestinal mechanics to displace gut bacterial symbionts. *Proceedings of the National Academy of Sciences*, *115*(16), E3779–E3787. https://doi.org/10.1073/pnas.1720133115

Ma, A. T., McAuley, S., Pukatzki, S., & Mekalanos, J. J. (2009). Translocation of a Vibrio cholerae Type VI Secretion Effector Requires Bacterial Endocytosis by Host Cells. *Cell Host & Microbe*, *5*(3), 234–243. https://doi.org/10.1016/j.chom.2009.02.005

Ma, A. T., & Mekalanos, J. J. (2010a). In vivo actin cross-linking induced by Vibrio cholerae type VI secretion system is associated with intestinal inflammation. *Proceedings of the National Academy of Sciences*, *107*(9), 4365–4370. https://doi.org/10.1073/pnas.0915156107

Ma, A. T., & Mekalanos, J. J. (2010b). In vivo actin cross-linking induced by Vibrio cholerae type VI secretion system is associated with intestinal inflammation. *Proceedings of the National Academy of Sciences of the United States of America*, *107*(9), 4365–4370. https://doi.org/10.1073/pnas.0915156107

McAleer, J. P., & Vella, A. T. (2008). Understanding How Lipopolysaccharide Impacts CD4 T-Cell Immunity. *Critical Reviews™ in Immunology*, *28*(4). https://doi.org/10.1615/CritRevImmunol.v28.i4.20

Melancon, E., De La Torre Canny, S. G., Sichel, S., Kelly, M., Wiles, T. J., Rawls, J. F., Eisen, J. S., & Guillemin, K. (2017). Best practices for germ-free derivation and gnotobiotic zebrafish husbandry. *Methods in Cell Biology*, *138*, 61–100. https://doi.org/10.1016/bs.mcb.2016.11.005

Milligan-Myhre, K., Charette, J. R., Phennicie, R. T., Stephens, W. Z., Rawls, J. F., Guillemin, K., & Kim, C. H. (2011). Study of Host–Microbe Interactions in Zebrafish. *Methods in Cell Biology*, *105*, 87–116. https://doi.org/10.1016/B978-0-12-381320-6.00004-7

Miyata, S., Kitaoka, M., Wieteska, L., Frech, C., Chen, N., & Pukatzki, S. (2010). The Vibrio Cholerae Type VI Secretion System: Evaluating its Role in the Human Disease Cholera. *Frontiers in Microbiology*, *1*. https://www.frontiersin.org/articles/10.3389/fmicb.2010.00117

Monjarás Feria, J., & Valvano, M. A. (2020). An Overview of Anti-Eukaryotic T6SS Effectors. *Frontiers in Cellular and Infection Microbiology*, *10*. https://www.frontiersin.org/articles/10.3389/fcimb.2020.584751

Muller, P. A., Koscsó, B., Rajani, G. M., Stevanovic, K., Berres, M.-L., Hashimoto, D., Mortha, A., Leboeuf, M., Li, X.-M., Mucida, D., Stanley, E. R., Dahan, S., Margolis, K. G., Gershon, M. D., Merad, M., & Bogunovic, M. (2014). Crosstalk between Muscularis Macrophages and Enteric Neurons Regulates Gastrointestinal Motility. *Cell*, *158*(2), 300–313. https://doi.org/10.1016/j.cell.2014.04.050

Noris, M., & Remuzzi, G. (2013). Overview of Complement Activation and Regulation. *Seminars in Nephrology*, *33*(6), 479–492. https://doi.org/10.1016/j.semnephrol.2013.08.001

Pang, B., Yan, M., Cui, Z., Ye, X., Diao, B., Ren, Y., Gao, S., Zhang, L., & Kan, B. (2007). Genetic Diversity of Toxigenic and Nontoxigenic Vibrio cholerae Serogroups O1 and O139 Revealed by Array-Based Comparative Genomic Hybridization. *Journal of Bacteriology*, *189*(13), 4837–4849. https://doi.org/10.1128/jb.01959-06

Pendse, M., De Selle, H., Vo, N., Quinn, G., Dende, C., Li, Y., Salinas, C. N., Srinivasan, T., Propheter, D. C., Crofts, A. A., Koo, E., Hassell, B., Ruhn, K. A., Raj, P., Obata, Y., & Hooper, L. V. (2023). Macrophages regulate gastrointestinal motility through complement component 1q. *eLife*, *12*, e78558. https://doi.org/10.7554/eLife.78558

Pukatzki, S., Ma, A. T., Revel, A. T., Sturtevant, D., & Mekalanos, J. J. (2007a). Type VI secretion system translocates a phage tail spike-like protein into target cells where it cross-links actin. *Proceedings of the National Academy of Sciences*, *104*(39), 15508–15513. https://doi.org/10.1073/pnas.0706532104

Pukatzki, S., Ma, A. T., Revel, A. T., Sturtevant, D., & Mekalanos, J. J. (2007b). Type VI secretion system translocates a phage tail spike-like protein into target cells where it cross-links actin. *Proceedings of the National Academy of Sciences*, *104*(39), 15508–15513. https://doi.org/10.1073/pnas.0706532104

Pukatzki, S., Ma, A. T., Sturtevant, D., Krastins, B., Sarracino, D., Nelson, W. C., Heidelberg, J. F., & Mekalanos, J. J. (2006). Identification of a conserved bacterial protein secretion system in Vibrio cholerae using the Dictyostelium host model system. *Proceedings of the National Academy of Sciences*, *103*(5), 1528–1533. https://doi.org/10.1073/pnas.0510322103

Rolig, A. S., Mittge, E. K., Ganz, J., Troll, J. V., Melancon, E., Wiles, T. J., Alligood, K., Stephens, W. Z., Eisen, J. S., & Guillemin, K. (2017). The enteric nervous system promotes intestinal health by constraining microbiota composition. *PLOS Biology*, *15*(2), e2000689. https://doi.org/10.1371/journal.pbio.2000689

Rolig, A. S., Parthasarathy, R., Burns, A. R., Bohannan, B. J. M., & Guillemin, K. (2015). Individual Members of the Microbiota Disproportionately Modulate Host Innate Immune Responses. *Cell Host & Microbe*, *18*(5), 613–620. https://doi.org/10.1016/j.chom.2015.10.009

Russell, A. B., Peterson, S. B., & Mougous, J. D. (2014). Type VI secretion system effectors: Poisons with a purpose. *Nature Reviews Microbiology*, *12*(2), Article 2. https://doi.org/10.1038/nrmicro3185

Samuel, B. S., Shaito, A., Motoike, T., Rey, F. E., Backhed, F., Manchester, J. K., Hammer, R. E., Williams, S. C., Crowley, J., Yanagisawa, M., & Gordon, J. I. (2008). Effects of the gut microbiota on host adiposity are modulated by the short-chain fatty-acid binding G protein-coupled receptor, Gpr41. *Proceedings of the National Academy of Sciences*, *105*(43), 16767–16772. https://doi.org/10.1073/pnas.0808567105

Sana, T. G., Lugo, K. A., & Monack, D. M. (2017). T6SS: The bacterial "fight club" in the host gut. *PLOS Pathogens*, *13*(6), e1006325. https://doi.org/10.1371/journal.ppat.1006325

Schwartz, K., Hammerl, J. A., Göllner, C., & Strauch, E. (2019). Environmental and Clinical Strains of Vibrio cholerae Non-O1, Non-O139 From Germany Possess Similar Virulence Gene Profiles. *Frontiers in Microbiology*, *10*. https://www.frontiersin.org/articles/10.3389/fmicb.2019.00733

Sehgal, A., Irvine, K. M., & Hume, D. A. (2021). Functions of macrophage colony-stimulating factor (CSF1) in development, homeostasis, and tissue repair. *Seminars in Immunology*, *54*, 101509. https://doi.org/10.1016/j.smim.2021.101509

Shiau, C. E., Kaufman, Z., Meireles, A. M., & Talbot, W. S. (2015). Differential requirement for irf8 in formation of embryonic and adult macrophages in zebrafish. *PloS One*, *10*(1), e0117513. https://doi.org/10.1371/journal.pone.0117513

Sit, B., Fakoya, B., & Waldor, M. K. (2022). Animal models for dissecting Vibrio cholerae intestinal pathogenesis and immunity. *Current Opinion in Microbiology*, *65*, 1–7. https://doi.org/10.1016/j.mib.2021.09.007

Son, M., Diamond, B., & Santiago-Schwarz, F. (2015). Fundamental role of C1q in autoimmunity and inflammation. *Immunologic Research*, *63*(1–3), 101–106. https://doi.org/10.1007/s12026-015-8705-6

Sorlien, E. L., Witucki, M. A., & Ogas, J. (2018). Efficient Production and Identification of CRISPR/Cas9-generated Gene Knockouts in the Model System Danio rerio. *JoVE (Journal of Visualized Experiments)*, *138*, e56969. https://doi.org/10.3791/56969

Stephens, W. Z., Wiles, T. J., Martinez, E. S., Jemielita, M., Burns, A. R., Parthasarathy, R., Bohannan, B. J. M., & Guillemin, K. (2015). Identification of Population Bottlenecks and Colonization Factors during Assembly of Bacterial Communities within the Zebrafish Intestine. *mBio*, *6*(6), e01163-01115. https://doi.org/10.1128/mBio.01163-15

Taormina, M. J., Jemielita, M., Stephens, W. Z., Burns, A. R., Troll, J. V., Parthasarathy, R., & Guillemin, K. (2012). Investigating Bacterial-Animal Symbioses with Light Sheet Microscopy. *The Biological Bulletin*, *223*(1), 7–20.

Thielicke, W., & Stamhuis, E. J. (2014). PIVlab – Towards User-friendly, Affordable and Accurate Digital Particle Image Velocimetry in MATLAB. *Journal of Open Research Software*, *2*. https://doi.org/10.5334/jors.bl

Vanden Broeck, D., Horvath, C., & De Wolf, M. J. S. (2007). Vibrio cholerae: Cholera toxin. *The International Journal of Biochemistry & Cell Biology*, *39*(10), 1771–1775. https://doi.org/10.1016/j.biocel.2007.07.005

Westerfield, M. (2000). *The Zebrafish Book: A Guide for the Laboratory Use of Zebrafish (Danio Rerio)*. University of Oregon Press.

Wiles, T. J., Jemielita, M., Baker, R. P., Schlomann, B. H., Logan, S. L., Ganz, J., Melancon, E., Eisen, J. S., Guillemin, K., & Parthasarathy, R. (2016). Host Gut Motility Promotes Competitive Exclusion within a Model Intestinal Microbiota. *PLOS Biology*, *14*(7), e1002517. https://doi.org/10.1371/journal.pbio.1002517

Wiles, T. J., Schlomann, B. H., Wall, E. S., Betancourt, R., Parthasarathy, R., & Guillemin, K. (2020). Swimming motility of a gut bacterial symbiont promotes resistance to intestinal expulsion and enhances inflammation. *PLOS Biology*, *18*(3), e3000661. https://doi.org/10.1371/journal.pbio.3000661

Wiles, T. J., Wall, E. S., Schlomann, B. H., Hay, E. A., Parthasarathy, R., & Guillemin, K. (2018). Modernized Tools for Streamlined Genetic Manipulation and Comparative Study of Wild and Diverse Proteobacterial Lineages. *mBio*, *9*(5), e01877-18, /mbio/9/5/mBio.01877-18.atom. https://doi.org/10.1128/mBio.01877-18

Wong, J. M. W., de Souza, R., Kendall, C. W. C., Emam, A., & Jenkins, D. J. A. (2006). Colonic Health: Fermentation and Short Chain Fatty Acids. *Journal of Clinical Gastroenterology*, *40*(3), 235.

Yu, Y., Yang, W., Li, Y., & Cong, Y. (2020). Enteroendocrine Cells: Sensing Gut Microbiota and Regulating Inflammatory Bowel Diseases. *Inflammatory Bowel Diseases*, *26*(1), 11–20. https://doi.org/10.1093/ibd/izz217

Zhao, L., Hu, P., Zhou, Y., Purohit, J., & Hwang, D. (2011). NOD1 activation induces proinflammatory gene expression and insulin resistance in 3T3-L1 adipocytes. *American Journal of Physiology-Endocrinology and Metabolism*, *301*(4), E587–E598. https://doi.org/10.1152/ajpendo.00709.2010